

Slip and Radiation Effects for Two-dimensional Oblique Stagnation Point Flow Towards a Stretching Surface in a Viscoelastic Fluid

by

Muhammad Noveel Sadiq



A dissertation submitted in partial fulfillment of the requirements
for the degree of Master of Philosophy in Mathematics

Supervised by

Prof. Dr. Muhammad Sajid

School of Natural Sciences (SNS)

National University of Sciences and Technology

Islamabad, Pakistan

2016


National University of Sciences & Technology**M.Phil THESIS WORK**

We hereby recommend that the dissertation prepared under our supervision by: MUHAMMAD NOVEEL SADIQ, Regn No. NUST201361955MSNS78013F Titled: Slip and Radiation Effects for Two-dimensional Oblique Stagnation Point Flow Towards a Stretching Surface in a Viscoelastic Fluid be accepted in partial fulfillment of the requirements for the award of **M.Phil** degree.

Examination Committee Members1. Name: DR. MERAJ MUSTAFA HASHMISignature: 2. Name: DR. MUHAMMAD ASIF FAROOQSignature: 

3. Name: _____

Signature: _____

4. Name: DR. NASIR ALISignature: Supervisor's Name: DR. MUHAMMAD SAJIDSignature: 


Head of Department

25/5/16
Date

COUNTERSIGNEDDate: 25/5/16


Dean/Principal

Dedicated

To

My Parents, Teachers and Friends

Acknowledgement

My thanks goes first to Almighty Allah, Who gives power to the weak and helps the helpless, The most Gracious and the Merciful.

Salawat and salam for Prophet Muhammad (PBUH) who brought us from darkness to brightness.

I would like to express sincere gratitude to my supervisor, Professor of Mathematics, International Islamic University Islamabad, Dr. Muhammad Sajid, for his many valuable suggestions, support, guidance and encouragement throughout my thesis and research work.

I also wish to express my appreciation to the principal of SNS, National University of Sciences and Technology, Islamabad, Dr. Azad A. Siddiqui for his valuable support and efforts for the students of his department.

I am thankful to Head of Department Mathematics, National University of Sciences and Technology Dr. Matloob Anwar for his valuable educational and moral support.

I am also thankful to all the faculty members at SNS for their kind attention and encouragement.

I especially thanks to the mentor of my studies, Principal GHSS Bassali, Dr. Muhammad Tahir Mehmood for his favour and guidance in pursuing my educational goals.

I am heartedly thankful to all my friends especially Baber Khokhar, Kamran Nawaz and Yasir Zameer who have been supportive along the way of accomplishing my thesis and making my time memorable.

Many thanks go to my family members also, my brother Adeel Sheikh, my sister and especially my mother for her generous support she provided me throughout my entire life and particularly through the process of pursuing this degree.

Muhammad Noveel Sadiq

Abstract

This dissertation investigates the slip and radiation effects for the flow and heat transfer analysis of a Walters-B fluid. It is assumed that flow impinges obliquely on a stretching surface. The mathematical model is developed by utilizing conservation laws of mass, momentum and energy. Similarity variables are invoked to transform partial differential equations into ordinary differential equations. The obtained nonlinear problems are solved by implementing two different numerical methods namely, a hybrid numerical method and a Legendre wavelet spectral collocation method. The velocity overshoot predicted through the hybrid solution is controlled by the combination of Legendre wavelet spectral collocation method and shooting method. The results are presented in graphs and tables and are discussed for the influence of pertinent parameters.

Preface

In the past two decades the non-Newtonian fluids received considerable importance due to their practical applications in industry and technology. Different constitutive relationships have been proposed to discuss the important characteristics exhibited by the non-Newtonian fluids. Among these the Walters-B fluid [1] is a subclass of the viscoelastic fluids. The governing equations of Walters-B fluid are nonlinear and have one order more than the Navier-Stokes equations. Furthermore, the leading order derivative term vanishes at the starting point of the integration. This complexity challenged mathematicians to develop methods that overcome this difficulty. Beard and Walters [1] solved the problem of the stagnation point flow by using perturbation method. They presented a two term solution of the problem and overshoot in the velocity is predicted by the perturbation solution for the first time. Frater [2] suggested that this overshoot in the boundary layer is due to the approximate solution. Ariel [3] proposed a hybrid numerical method that combines the features of finite difference and shooting methods to solve the stagnation point flow of Walters-B fluid. In another paper Ariel [4] implemented generalized Gear's method and reported the same solution. Labropulu et. al. [5-10] solved different aspects of the boundary layer flow of Walters-B fluid using hybrid method. In a recent article Hussain et. al. [11] discussed the oblique stagnation point flow in Walters-B fluid towards a stretching sheet. In present dissertation we extended the problem of Hussain et. al. [11] by incorporating slip [12] and radiation effects [13]. Both hybrid method proposed by Ariel [3] and Legendre wavelet spectral collocation method [14] together with shooting method [15] are utilized to obtain the solution. The dissertation is structured as follow:

In chapter 1 basic definitions, governing equations and numerical methods are presented. Chapter 2 is denoted for the detailed review of the paper by Hussain et. al. [11]. The slip and radiation effects are presented in Chapter 3 using hybrid numerical method. In Chapter 4 the Legendre wavelets spectral collocation method is implemented to discuss the slip and radiation effects for stagnation point flow of a Walters-B fluid past a stretching sheet.

Contents

1	Fundamentals of fluid mechanics	1
1.1	Introduction	1
1.2	Fundamental concepts	1
1.2.1	Flow	1
1.2.2	Fluid	1
1.2.3	Pressure	2
1.2.4	Density	2
1.2.5	Stress	2
1.2.6	Viscosity	2
1.2.7	Boundary layer	3
1.2.8	Boundary layer thickness	3
1.2.9	Stagnation point	3
1.2.10	Newtonian fluids	4
1.2.11	Non-Newtonian fluids	4
1.2.12	Viscoelastic fluid	4
1.2.13	Prandtl number	4
1.3	Classification of fluid flows	5
1.3.1	Steady flow	5
1.3.2	Unsteady flow	5
1.3.3	Uniform flow	5
1.3.4	Non-uniform flow	5
1.3.5	Laminar flow	5
1.3.6	Turbulent flow	5
1.3.7	Rotational flow	6
1.3.8	Irrotational flow	6
1.3.9	Incompressible flow	6
1.3.10	Compressible flow	6
1.4	Assumptions for fluid flow	6

1.4.1	Conservation of mass	7
1.4.2	Conservation of momentum	7
1.4.3	Conservation of energy	8
1.5	Boundary conditions	8
1.5.1	No-slip boundary condition	8
1.5.2	Slip boundary condition	8
1.6	Method used for solution	9
1.6.1	Shooting method	9
1.6.2	Hybrid numerical method	10
1.6.3	Legendre wavelet spectral collocation method	13
2	Hybrid numerical method in stagnation-point flow of a viscoelastic fluid	18
2.1	Formulation of mathematical equations	18
2.1.1	Transformation from PDE to ODE	21
2.1.2	Skin friction	22
2.2	Numerical results and discussion	23
3	Slip and radiation effects for two-dimensional oblique stagnation point flow towards a stretching surface in a viscoelastic fluid by using hybrid method	29
3.1	Mathematical formulation	29
3.1.1	Slip condition	29
3.1.2	Energy equation	30
3.2	Numerical results and discussion	32
4	A Legendre wavelet spectral collocation method for two-dimensional oblique stagnation point flow of Walters-B fluid with heat transfer	44
4.1	Solution by the Legendre wavelet spectral collocation method	44
4.2	Numerical results and discussion	46
5	Conclusions	60
	Bibliography	60

Chapter 1

Fundamentals of fluid mechanics

1.1 Introduction to fluid mechanics

Fluid mechanics deals with the study of all fluids under static and dynamic situations. It deals with a relationship between forces, motions and statical conditions in a continuous material. The fluid mechanics study involves many fields that have no clear boundaries between them. Researchers distinguish between orderly and chaotic flow as the laminar and the turbulent flow. The objective of present chapter is to introduce the readers with the basic concepts of fluid mechanics. These basic details are vital in studying the fluid flow phenomenon presented in this dissertation.

1.2 Fundamental concepts

1.2.1 Flow

When a force acts on a substance, it undergoes deformation. If the deformation of substance takes place continuously, then the phenomenon is called a flow.

1.2.2 Fluid

If a substance deforms continuously under the effect of tangential forces (shear stresses) then substance is called a fluid. All liquids, gases, plasmas and to some extent plastic solids are fluids.

1.2.3 Pressure

Force per unit area acting normal to the surface is called pressure. It is a scalar quantity. Mathematically

$$p = \frac{F_n}{A} = \frac{dF_n}{dA}, \quad (1.1)$$

where F_n is the magnitude of the normal direction force and A is the cross sectional area. No change occurs in pressure by changing the orientation of surface elements.

1.2.4 Density

Density is the mass per unit volume of a substance at a given pressure and temperature. It is denoted by ρ and in mathematical terms can be written as

$$\rho = \frac{m}{V}. \quad (1.2)$$

The SI unit of density is $\frac{kg}{m^3}$.

1.2.5 Stress

If a body for example fluid, is deformable then the stress is the internal force acting on that deformable body. Quantitatively, stress is the amount of average force per unit area of a control volume within the deformable body.

Shear stress

The stress applied in tangential direction is called tangential or shear stress.

Normal stress

The stress applied in normal direction is the normal or tensile stress.

1.2.6 Viscosity

When a stress is applied to a deformable body it deforms and resists the applied stress. This resistance is known as viscosity. Viscosity is used to measure the degree of internal friction in the fluid.

Dynamic viscosity

Dynamic viscosity also known as absolute viscosity is the ratio of shear stress τ to the rate of deformation $\partial u/\partial y$. Mathematically,

$$\mu = \frac{\tau}{\partial u/\partial y}. \quad (1.3)$$

The unit of dynamic viscosity is $\frac{kg}{ms}$.

Kinematic viscosity

Kinematic viscosity also known as relative viscosity is rate at which momentum is transferred through a fluid. It is the ratio of absolute viscosity μ to the density ρ and is denoted by ν . Mathematically,

$$\nu = \frac{\mu}{\rho}. \quad (1.4)$$

The unit of kinematic viscosity is $\frac{m^2}{s}$.

1.2.7 Boundary layer

The boundary layer is a very thin layer of the fluid over the surface. The resistance or viscosity is maximum near the surface. As one moves away from the surface the effect of viscosity reduces and after a thin region above the surface this effect is negligible. Layer of the fluid inside the boundary layer moves faster than that near to the surface. At the top of the boundary layer the velocity of fluid particles is same as that of velocity of fluid particles outside the boundary layer. This velocity is called free stream velocity.

1.2.8 Boundary layer thickness

The distance from the surface to the fluid layer that attains a free stream velocity is termed as boundary layer thickness. It is denoted by δ .

1.2.9 Stagnation point

If there exists a point in the flow field where the velocity of the fluid becomes zero is called a stagnation point.

1.2.10 Newtonian fluids

Fluids in which shear stress is directly and linearly proportional to the deformation rate are called Newtonian fluids. For unidirectional flow,

$$\tau = \mu \frac{du}{dy}. \quad (1.5)$$

This law is known as Newton's law of viscosity. Water, oil and air are some examples of such fluids. It is important to mention that for Newtonian fluids viscosity is constant.

1.2.11 Non-Newtonian fluids

If the relation between the shear stress and deformation rate is non linear, we call the fluid as non-Newtonian fluid. In mathematical terms,

$$\tau = k \left(\frac{du}{dy} \right)^n, \quad (1.6)$$

where k is consistency index and n is flow behavior index. Eq. (1.6) can be written as

$$\tau = k \left(\frac{du}{dy} \right)^{n-1} \frac{du}{dy} = \eta \frac{du}{dy}, \quad (1.7)$$

where η is apparent viscosity. Tooth paste, shampoo, blood, paint, gel etc. are some examples of non-Newtonian fluids. The viscosity for a non-Newtonian fluid is not constant and is a function of shear stress.

1.2.12 Viscoelastic fluids

Viscoelastic fluids are the materials that exhibit both viscous and elastic characteristics when undergoing deformation. Honey and all polymer solutions are examples of the viscoelastic fluids.

1.2.13 Prandtl number

The Prandtl number is a dimensionless number defined as the ratio of viscous diffusivity to thermal diffusivity, i.e. the Prandtl number is given as

$$Pr = \frac{\nu}{\alpha} = \frac{\mu c_p}{k}, \quad (1.8)$$

where c_p is the specific heat and k is the thermal conductivity.

1.3 Classification of fluid flows

In every fluid some parameters associated with it vary when fluid is moving. The variation in the parameters may be with respect to time or space coordinates. Based on these variations in the parameters we can classify the fluid flows.

1.3.1 Steady flow

If the flow parameters or properties do not vary with respect to time, we say flow is steady.

1.3.2 Unsteady flow

If the flow parameter or properties are function of time and change when time changes, we call the flow as unsteady.

1.3.3 Uniform flow

If the flow properties remain constant along the flow path, we say that flow is uniform.

1.3.4 Non-uniform flow

If the flow properties are different at different points of space, we say that flow is non-uniform.

1.3.5 Laminar flow

If a fluid is flowing in such a way that each particle of fluid has a definite path and the path of particles do not intersect we call it as a laminar flow.

1.3.6 Turbulent flow

As the speed of fluid flow increases the intersection between different layers occurs and thus smoothness of layers is destroyed and flow becomes turbulent.

1.3.7 Rotational flow

If the particles of the fluid are in angular motion we say that flow is rotational. For such flow

$$\nabla \times \mathbf{V} \neq \mathbf{0}, \quad (1.9)$$

where \mathbf{V} is velocity field.

1.3.8 Irrotational flow

If there is no angular motion present we say that flow is irrotational. For such flow

$$\nabla \times \mathbf{V} = \mathbf{0}. \quad (1.10)$$

1.3.9 Incompressible flow

If the volume of given fluid particles remain constant i.e. the density of the fluid is constant, the flow is classified as incompressible flow. Generally, all liquids are incompressible fluids.

1.3.10 Compressible flow

If the volume of the fluid particles varies with space and time i.e. the density is function of space and time and no more constant, the flow is said to be compressible. All gases are compressible fluids.

1.4 Assumptions for fluid flow

To study a fluid flow one has to make some basic assumptions which as a result turn into equations. The analysis of any problem in fluid mechanics necessarily has the following assumptions.

1. Conservation of mass
2. Conservation of momentum
3. Conservation of energy

it is not necessary to consider all the basic laws to study one specific problem. Moreover, in certain situations one has to bring additional relations describing physical properties of fluids under certain given conditions.

1.4.1 Conservation of mass (continuity equation)

The law of conservation of mass for compressible flow is given by

$$\frac{\partial \rho}{\partial t} + \nabla \cdot (\rho \mathbf{V}) = 0, \quad (1.11)$$

for steady and incompressible flow conservation of mass is given by

$$\nabla \cdot \mathbf{V} = 0. \quad (1.12)$$

In Cartesian coordinates, the component form of the continuity equation is

$$\frac{\partial u}{\partial x} + \frac{\partial v}{\partial y} + \frac{\partial w}{\partial z} = 0, \quad (1.13)$$

in which u, v, w are the velocity components in x, y, z directions respectively.

1.4.2 Conservation of momentum

The conservation of momentum is expressed by the relation

$$\rho \left[\frac{\partial \mathbf{V}}{\partial t} + (\mathbf{V} \cdot \nabla) \mathbf{V} \right] = -\nabla p + \nabla \cdot \mathbf{T} + \rho \mathbf{b}, \quad (1.14)$$

where p is the pressure, \mathbf{T} is the Cauchy stress tensor and \mathbf{b} is the body force per unit volume. In absence of body forces the momentum equations for a viscous fluid in Cartesian coordinates are

$$\rho \left(\frac{\partial u}{\partial t} + u \frac{\partial u}{\partial x} + v \frac{\partial u}{\partial y} + w \frac{\partial u}{\partial z} \right) = -\frac{\partial p}{\partial x} + \mu \left(\frac{\partial^2 u}{\partial x^2} + \frac{\partial^2 u}{\partial y^2} + \frac{\partial^2 u}{\partial z^2} \right), \quad (1.15)$$

$$\rho \left(\frac{\partial v}{\partial t} + u \frac{\partial v}{\partial x} + v \frac{\partial v}{\partial y} + w \frac{\partial v}{\partial z} \right) = -\frac{\partial p}{\partial y} + \mu \left(\frac{\partial^2 v}{\partial x^2} + \frac{\partial^2 v}{\partial y^2} + \frac{\partial^2 v}{\partial z^2} \right), \quad (1.16)$$

$$\rho \left(\frac{\partial w}{\partial t} + u \frac{\partial w}{\partial x} + v \frac{\partial w}{\partial y} + w \frac{\partial w}{\partial z} \right) = -\frac{\partial p}{\partial z} + \mu \left(\frac{\partial^2 w}{\partial x^2} + \frac{\partial^2 w}{\partial y^2} + \frac{\partial^2 w}{\partial z^2} \right). \quad (1.17)$$

1.4.3 Conservation of energy

Law of conservation of energy is given by

$$\rho c_p \left[\frac{\partial T}{\partial t} + (\mathbf{V} \cdot \nabla) T \right] = k \nabla^2 T + \nabla \cdot \mathbf{q} + \boldsymbol{\tau} : \nabla \mathbf{V} + Q, \quad (1.18)$$

where T is the temperature, k is thermal conductivity, \mathbf{q} is the radiative heat flux, c_p is the specific heat and Q is the heat source or sink. In component form the heat equation becomes

$$\begin{aligned} \frac{\partial T}{\partial t} + u \frac{\partial T}{\partial x} + v \frac{\partial T}{\partial y} = & \frac{k}{\rho c_p} \left(\frac{\partial^2 T}{\partial x^2} + \frac{\partial^2 T}{\partial y^2} \right) - \frac{1}{\rho c_p} \frac{\partial q_r}{\partial y} + \frac{2\mu}{\rho c_p} \left\{ \left(\frac{\partial u}{\partial x} \right)^2 \right. \\ & \left. + \left(\frac{\partial v}{\partial y} \right)^2 \right\} + \frac{\mu}{\rho c_p} \left\{ \left(\frac{\partial u}{\partial y} + \frac{\partial v}{\partial x} \right)^2 \right\} + \frac{Q}{\rho c_p} (T - T_\infty), \end{aligned} \quad (1.19)$$

where q_r is the radiative heat flux, T and T_∞ respectively are fluid temperatures within the boundary layer and in the free stream.

1.5 Boundary conditions

Boundary conditions are very important to discuss the mathematical solution of the equations governing a particular flow problem. Boundary condition is a set of conditions that must be satisfied at the region in which a system of differential equations is to be solved.

1.5.1 No-slip boundary condition

If a fluid is flowing over a solid surface, the no slip boundary condition states that the fluid will have zero velocity relative to the boundary i.e. there is no relative motion between fluid and the solid surface.

1.5.2 Slip boundary condition

Slip boundary condition states that the fluid velocity at the surface is proportional to the shear stress at the surface. Mathematically,

$$\mu v_s = b \tau_s, \quad (1.20)$$

where b is the slip length. v_s and τ_s are velocity and shear stress at the surface respectively. The slip length b is the distance inside the surface where the velocity is zero.

1.6 Method used for solution

Here we will explain numerical techniques we have used to solve the governing equations in next chapters.

1.6.1 Shooting method

Shooting method [15] is one of the iterative techniques used for boundary value problems. First we reduce boundary value problem into a system of first order initial value problems. A guess is made for the missing initial condition then we find the solution of initial value problem instead of boundary value problem. Let us consider a second order boundary value problem.

$$\frac{d^2y}{dx^2} = f\left(x, y, \frac{dy}{dx}\right), \quad (1.21)$$

with boundary condition

$$y(0) = 0, \quad y(L) = A, \quad (1.22)$$

where f is an arbitrary function and data is prescribed at $x = 0$ and $x = L$. To solve the boundary value problem we reduce it into a system of first order differential equations as

$$\frac{dy}{dx} = u, \quad \frac{du}{dx} = f(x, y, u), \quad (1.23)$$

with initial conditions

$$y(0) = 0, \quad y'(0) = u(0) = s, \quad (1.24)$$

where s denotes the missing initial condition which will be assigned an initial value. If we denote the solutions of initial value problem as $y(x, s)$ and $u(x, s)$, we can search the value of s such that

$$y(L, s) - A = 0 = \phi(s). \quad (1.25)$$

Here one can use Newton's formula to find the value of s as follow

$$s^{(n+1)} = s^{(n)} - \frac{\phi(s^{(n)})}{\frac{d\phi(s^{(n)})}{ds}}, \quad (1.26)$$

which implies that

$$s^{(n+1)} = s^{(n)} - \frac{y(L, s^{(n)}) - A}{\frac{\partial y(L, s^{(n)})}{\partial s}}. \quad (1.27)$$

To find the derivative of y w.r.t. s we differentiate the system of equations w.r.t s and get

$$\frac{dY}{dx} = U, \quad \frac{dU}{dx} = \frac{\partial f}{\partial y}Y + \frac{\partial f}{\partial u}U, \quad (1.28)$$

where

$$Y = \frac{\partial y}{\partial s}, \quad U = \frac{\partial u}{\partial s}, \quad (1.29)$$

initial condition becomes

$$Y(0) = 0, \quad U(0) = 1. \quad (1.30)$$

The solution of Eq. (1.21) with boundary condition (1.22) can therefore be obtained by applying the following steps:

1. We choose the initial guess for the missing initial condition (1.24) and denote it by $s^{(1)}$.
2. We solve the system of Eqs. (1.23) subject to initial conditions (1.24) from $x = 0$ to $x = L$.
3. We Integrate the system of Eqs.(1.28) subject to initial condition (1.30) from $x = 0$ to $x = L$.
4. Substituting the value of $y(L, s^{(1)})$ obtained by step (2) and $Y(L, s^{(1)})$ obtained by step (3) into Eq. (1.29) as

$$s^{(2)} = s^{(1)} - \frac{y(L, s^{(1)}) - A}{\frac{\partial y(L, s^{(1)})}{\partial s}}, \quad (1.31)$$

so next approximation of missing initial condition $s^{(2)}$ is obtained.

5. We repeat steps until value of s is in specified degree of accuracy.

1.6.2 Hybrid numerical method

This hybrid numerical method was introduced by P.D. Ariel [3] in 1992 for computing the flow of viscoelastic and second-order fluids. This method is a combination of finite difference technique and the shooting method [15]. Here

we applied this method to obtain the numerical solution to the flow problem of the Walters-B fluid. A classical example of this method is the analysis of the two-dimensional flow of Walters-B fluid at a stagnation point given by Beard and Walters [1]. The governing equation of motion in form of non-linear ordinary differential equation in F is

$$F''' + FF'' - F'^2 + 1 + K(FF'' - 2F'F''' + F''^2) = 0, \quad (1.32)$$

with the boundary conditions

$$F(0) = 0, \quad F'(0) = 0, \quad F'(\infty) = 1, \quad (1.33)$$

Beard and Walters [1] investigated the solution of the problem (1.32) by assuming

$$F = F_0 + kF_1. \quad (1.34)$$

The differential equations obtained for both F_0 and F_1 are of third order and their solution can be obtained by using the any standard integration technique. It was observed that the velocity in the boundary layer exceeds the mainstream velocity. Due to phenomenon of overshoot in velocity this problem attracted considerable attention and has been attempted by different researchers using different numerical techniques. Frater [2] argued that the velocity overshoot is due to seeking a regular perturbation solution for the problem. He did not present the velocity profiles in his work, so that the question of velocity overshoot in boundary layer remained unanswered. Further it can be seen that there is a singularity at $y = 0$. Secondly, the initial value problem becomes highly unstable numerically for $K \rightarrow 0$ so simple integration techniques cannot be applicable. In 1992 P.D. Arial [3] solved the problem (1.32) by using a hybrid method which combines the finite difference technique and the shooting method [15]. The central difference technique is used to increase the accuracy of the solution.

Let us assume

$$F''(0) = s, \quad (1.35)$$

then equation (1.32) can be treated as an initial value problem and value of s can be obtained by shooting method such that (1.33) is satisfied. We find the values of $F'''(0)$ which is extra condition to solve the Eq. (1.32) by substituting the initial condition in (1.32), we get

$$F'''(0) = -(1 + Ks^2), \quad (1.36)$$

Let

$$y_1 = F, \quad y_2 = F', \quad y_3 = F'', \quad y_4 = y_3' = F''', \quad y_3'' = F^{iv}, \quad (1.37)$$

then Eqs. (1.32)- (1.33) can be written as

$$y_3' + y_1 y_3 - y_2^2 + 1 + K(y_1 y_3'' - 2y_2 y_3' - y_3^2) = 0, \quad (1.38)$$

$$y_1(0) = 0, \quad y_2(0) = 0, \quad y_3(0) = s, \quad y_3'(0) = -(1 + Ks^2), \quad y_2(\infty) = 1. \quad (1.39)$$

Let us introduce a mesh defined $y_i = ih$, $i = 1, 2, \dots, N$. We will replace the 1st and 2nd derivatives in Eq. (1.38) by following the central difference formulas

$$y_3' = \frac{y_3^{j+1} - y_3^{j-1}}{h} \quad y_3'' = \frac{y_3^{j+1} - 2y_3^j + y_3^{j-1}}{h^2}, \quad (1.40)$$

which leads the system of equations

$$y_3^{j+1} = \left(1 + \frac{2K}{h} y_1^j - 2K y_2^j\right)^{-1} \left[y_3^{j-1} - 2h [y_1^j y_3^j + 1 - (y_2^j)^2] - K \left(2y_1^j \frac{y_3^{j-1} - 2y_3^j}{h} + 2y_2^j y_3^{j-1} + 2h (y_3^j)^2 \right) \right], \quad (1.41)$$

$$y_2^{j+1} = y_2^j + \frac{1}{2} h (y_3^j + y_3^{j+1}), \quad (1.42)$$

$$y_1^{j+1} = y_1^j + \frac{1}{2} h (y_2^j + y_2^{j+1}), \quad (1.43)$$

boundary conditions (1.33) becomes

$$y_1^0 = 0 \quad y_2^0 = 0 \quad y_2^N = 1. \quad (1.44)$$

We obtain the value of y_3^1 by expanding y_3^1 in Taylor Series around $y = 0$. We have

$$y_3^1 = y_3^0 + h(y_3^0)' + \frac{h^2}{2!}(y_3^0)'' + \dots, \quad (1.45)$$

or

$$y_3^1 = F''(0) + hF'''(0) + \frac{h^2}{2!}F^{iv}(0) + \dots \quad (1.46)$$

To obtain the value of $F^{iv}(0)$ we differentiate Eq. (1.32) and set $y = 0$. We have

$$F^{iv}(0) = 0, \quad (1.47)$$

therefore

$$y_3^1 = s - h(1 + ks^2). \quad (1.48)$$

Now we first choose an approximate value of $F''(0) = s$ and y_3^1 is calculated from Eq. (1.48). Then y_2^1 and y_1^1 are calculated from Eqs. (1.42) and (1.43). Then y_3^2 is calculated from Eq. (1.43). Then y_2^2 and y_1^2 are calculated from Eqs. (1.42) and (1.43). Repeat the cycle until the values of $y_1, y_2,$ and y_3 have been calculated at all the mesh points. The values of s is modified by using the secant method defined by

$$s_{n+1} = s_n + (1 - F'(\infty, s_n)) \frac{s_n - s_{n-1}}{F'(\infty, s_n) - F'(\infty, s_{n-1})}. \quad (1.49)$$

This process is repeated so that we can get a solution of desired accuracy.

1.6.3 Legendre wavelet spectral collocation method

This is an iterative method for solving differential equations with initial values on large intervals. In this method, we extend the Legendre wavelet suitable for large intervals and then the Legendre-Gauss collocation points of the Legendre wavelets are derived. The iterative spectral method converts the differential equation to a set of algebraic equations. By solving these algebraic equations we get an approximate solution for the differential equation.

Let us consider the initial value problem

$$F(x, y(x), y'(x), \dots, y^{(l-1)}(x), y^{(l)}(x)) = 0, \quad x \in [0, T], \quad (1.50)$$

with the initial conditions

$$y(x_0) = y_0, \dots, y^{(l-1)}(x_0) = y_0^{(l-1)}, \quad (1.51)$$

on large domain $[0, T)$. Discrete wavelet transform is defined as

$$\psi_{m,n}(t) = a^{-m/2} \psi(a^{-m}t - nb), \quad (1.52)$$

where a^m is the scale and $na^m b$ is the shift for any $m, n \in \mathbb{Z}$ and ψ is derived from Legendre polynomial. $\psi_{m,n}(t)$ depends on five arguments (k, T, n, m, t) , T is large integer, m is order of the Legendre polynomial, t stands for the normalized time.

$$k = 1, 2, \dots, T, \quad n = 1, 2, \dots, 2^{k-1}T. \quad (1.53)$$

We define the Legendre wavelets on the intervals $[0, T)$ by

$$\psi_{m,n}(t) = \begin{cases} (m + \frac{1}{2})^{1/2} 2^{k/2} L_m(2^k t - 2n + 1), & \frac{n-1}{2^{k-1}} \leq t < \frac{n}{2^{k-1}}, \\ 0, & \text{otherwise} \end{cases} \quad (1.54)$$

$L_m(t)$ is m th-order Legendre polynomial with orthogonal weight function $w(t) = 1$. By recursive formulas Legendre polynomials are obtained.

$$\begin{aligned} L_0(t) &= 1, \\ L_1(t) &= t, \\ L_{m+1}(t) &= \frac{2m+1}{m+1} t L_m(t) - \frac{m}{m+1} L_{m-1}(t), \quad m = 1, 2, 3, \dots \end{aligned} \quad (1.55)$$

Legendre-Gauss collocation points $x_0 < x_1 < x_2 \dots < x_{m-1}$ are roots of the $L_m(x)$ in $(-1, 1)$ and $\{w_j\}_{j=0}^{m-1}$ are corresponding weights and

$$w_j = \frac{2}{(1-x_j^2)(L'_M(x_j))^2}, \quad j = 0, 1, \dots, M-1. \quad (1.56)$$

Any function $f(x)$ can be extended in term of Legendre wavelets as

$$f(x) = \sum_{n=1}^{\infty} \sum_{m=0}^{\infty} y_{n,m} \psi_{n,m}(x) \quad (1.57)$$

where $y_{n,m}$ can be approximated to

$$y_{n,m} \simeq \sum_{j=0}^{M-1} \bar{w}_j f(x_{nj}) \psi_{n,m}(x_{nj}), \quad (1.58)$$

where

$$\bar{w}_j = \frac{w_j}{2^k}, \quad x_{nj} = \frac{x_j}{2^k} + \frac{2n-1}{2^k}, \quad (1.59)$$

$$j = 0, 1, \dots, M-1, \quad n = 1, 2, \dots, 2^{k-1}T. \quad (1.60)$$

so Eq.(1.55) becomes

$$f(x) \simeq \sum_{n=1}^{\infty} \sum_{m=0}^{\infty} \sum_{j=0}^{M-1} \bar{w}_j f(x_{nj}) \psi_{n,m}(x_{nj}) \psi_{n,m}(x), \quad (1.61)$$

since

$$\sum_{n=1}^{\infty} \sum_{m=0}^{\infty} \psi_{n,m}(x) \psi_{n,m}(t) = \delta(x-t), \quad (1.62)$$

is identity so truncating $M-1, 2^{k-1} T$ and introducing

$$I_{nj}(x) = \sum_{m=0}^{M-1} \bar{w}_j \psi_{n,m}(x_{nj}) \psi_{n,m}(x), \quad (1.63)$$

we have

$$f(x) \simeq \sum_{n=1}^{2^{k-1}T} \sum_{j=0}^{M-1} I_{nj}(x) f(x_{nj}). \quad (1.64)$$

Solving IVPs on a large domain

Consider the problem (1.48) with initial condition (1.49). We divide the interval $[0, T)$ into subintervals given by

$$\left[\frac{n-1}{2^{k-1}}, \frac{n}{2^{k-1}} \right), \quad (1.65)$$

for $n = 1, 2, \dots, 2^{k-1}T$. As a result, $x \in \left[\frac{n-1}{2^{k-1}}, \frac{n}{2^{k-1}} \right)$ implies that

$$\psi_{pj}(x) = 0 \quad \text{for any } p \neq n. \quad (1.66)$$

Thus, $I_{pj}(x) = 0$ for all $p \neq n$. Consequently, the Legendre wavelet interpolant approximation to the function y on the n th subinterval follows (1.64) and is given by

$$y(x) \simeq Y_n(x)$$

$$= \sum_{p=1}^{2^{k-1}T} \sum_{j=0}^{M-1} I_{pj}(x) y_{pj}(x) \quad (1.67)$$

$$= \sum_{j=0}^{M-1} I_{nj}(x) y_{nj}(x), \quad \text{for } x \in \left[\frac{n-1}{2^{k-1}}, \frac{n}{2^{k-1}} \right). \quad (1.68)$$

We define

$$Y_n^{(s)}(x) = \sum_{j=0}^{M-1} I_{nj}^{(s)}(x) y_{nj}(x), \quad s = 1, 2, \dots, m. \quad (1.69)$$

Applying the points $\{x_{nj} \mid n = 1, 2, \dots, 2^{k-1}T, j = l, \dots, M-1\}$ into Eq. (1.48) we obtain

$$F\left(x_{nj}, Y_n(x_{nj}), Y_n'(x_{nj}), \dots, Y_n^{(l-1)}(x_{nj}), Y_n^l(x_{nj})\right) = 0, \quad (1.70)$$

moreover, for the n th subinterval the initial conditions for any $s = 0, \dots, l-1$ can be written as follow

$$\lim_{x \rightarrow \left(\frac{n-1}{2^{k-1}}\right)^-} Y_n^{(s)}(x) - Y_n^{(s)}\left(\frac{n-1}{2^{k-1}}\right) = 0. \quad (1.71)$$

Equations (1.70) and (1.71) give a system of M algebraic equations. By solving this system of algebraic equations we obtain $\{y_{nj} \mid n = 1, 2, \dots, 2^{k-1}T, j = 0, \dots, M-1\}$. We obtain the approximate solution on the n th subinterval by substituting y_{nj} into Eq. (1.67).

We start the procedure by setting $n = 1$ and the initial conditions (1.51) are used to obtain the approximate solution for the first subinterval $[0, 1/2^{k-1})$. We obtain the initial conditions for second subinterval from equation (1.71).

Consequently, an approximate solution for the second subinterval is computed. Similar procedure is followed to compute the approximate solution for all subintervals. Finally, the approximate solution for the initial value problem (1.50) with initial conditions (1.51) on the whole domain $[0, T)$ is obtained and is given by

$$y(x) \simeq \sum_{n=1}^{2^{k-1}T} Y_n(x) = \sum_{n=1}^{2^{k-1}T} \sum_{j=0}^{M-1} I_{nj}(x) y_{nj}(x). \quad (1.72)$$

Chapter 2

Hybrid numerical method in stagnation-point flow of a viscoelastic fluid

This chapter contains the details of the steady, incompressible two-dimensional oblique stagnation-point flow of Walters-B fluid over a stretching plate discussed by Labropulu et al. [11]. The behavior inside the boundary layer of Walters-B fluid for various values of the viscoelastic parameter is investigated. The governing partial differential equations are reduced into a system of coupled dimensionless ordinary differential equations by using similarity transformations. A numerical solution of the governing equations is obtained by using a hybrid numerical method [3] which combines the features of finite difference and shooting methods.

2.1 Formulation of mathematical equations

Consider the steady, incompressible two-dimensional oblique stagnation-point flow of Walters-B fluid towards a stretching surface at $\bar{y} = 0$. Cartesian coordinates are (\bar{x}, \bar{y}) such that the \bar{x} -axis being along the surface and the \bar{y} -axis perpendicular to the surface. The constitutive equation for Walters-B fluid is

$$\mathbf{T} = -p\mathbf{I} + \boldsymbol{\tau}, \quad (2.1)$$

where $\boldsymbol{\tau}$ is the extra stress tensor defined by [1]

$$\boldsymbol{\tau} = \mu\mathbf{A}_1 - k_0\bar{\boldsymbol{\tau}}, \quad (2.2)$$

in which k_0 is fluid viscoelasticity and first Rivlin-Ericksen tensor \mathbf{A}_1 is defined as

$$\mathbf{A}_1 = \mathbf{L} + \mathbf{L}^T, \quad (2.3)$$

in which

$$\mathbf{L} = \text{grad } \bar{\mathbf{V}}, \quad (2.4)$$

and

$$\bar{\boldsymbol{\tau}} = \frac{\partial \mathbf{A}_1}{\partial t} + (\bar{\nabla} \cdot \bar{\nabla}) \mathbf{A}_1 - \mathbf{A}_1 \mathbf{L} - \mathbf{L}^T \mathbf{A}_1 + (\bar{\nabla} \cdot \bar{\mathbf{V}}) \mathbf{A}_1, \quad (2.5)$$

Substituting (2.2) - (2.5) in (2.1) we have

$$\mathbf{T} = -p\mathbf{I} + \mu\mathbf{A}_1 - k_0 \left(\frac{\partial \mathbf{A}_1}{\partial t} + (\bar{\nabla} \cdot \bar{\nabla}) \mathbf{A}_1 - \mathbf{A}_1 \mathbf{L} - \mathbf{L}^T \mathbf{A}_1 + (\bar{\nabla} \cdot \bar{\mathbf{V}}) \mathbf{A}_1 \right). \quad (2.6)$$

For two dimensional flow we have the following velocity field

$$\bar{\mathbf{V}} = [\bar{u}(\bar{x}, \bar{y}), \bar{v}(\bar{x}, \bar{y}), 0]. \quad (2.7)$$

Substituting (2.6) and (2.7) into Eqs. (1.11) and (1.13), one obtains the following equations in component form

$$\frac{\partial \bar{u}}{\partial \bar{x}} + \frac{\partial \bar{v}}{\partial \bar{y}} = 0, \quad (2.8)$$

$$\begin{aligned} \bar{u} \frac{\partial \bar{u}}{\partial \bar{x}} + \bar{v} \frac{\partial \bar{u}}{\partial \bar{y}} = & -\frac{1}{\rho} \frac{\partial \bar{p}}{\partial \bar{x}} + \nu \bar{\nabla}^2 \bar{u} - \frac{k_0}{\rho} \left[\frac{\partial}{\partial \bar{x}} \left[2\bar{u} \frac{\partial^2 \bar{u}}{\partial \bar{x}^2} + 2\bar{v} \frac{\partial^2 \bar{u}}{\partial \bar{x} \partial \bar{y}} + 4 \left(\frac{\partial \bar{u}}{\partial \bar{x}} \right)^2 \right. \right. \\ & \left. \left. + 2 \frac{\partial \bar{v}}{\partial \bar{x}} \left(\frac{\partial \bar{v}}{\partial \bar{x}} + \frac{\partial \bar{u}}{\partial \bar{y}} \right) \right] + \frac{\partial}{\partial \bar{y}} \left[\left(\bar{u} \frac{\partial}{\partial \bar{x}} + \bar{v} \frac{\partial}{\partial \bar{y}} \right) \left(\frac{\partial \bar{v}}{\partial \bar{x}} + \frac{\partial \bar{u}}{\partial \bar{y}} \right) + 2 \frac{\partial \bar{u}}{\partial \bar{x}} \frac{\partial \bar{u}}{\partial \bar{y}} + 2 \frac{\partial \bar{v}}{\partial \bar{x}} \frac{\partial \bar{v}}{\partial \bar{y}} \right] \right], \quad (2.9) \end{aligned}$$

$$\begin{aligned} \bar{u} \frac{\partial \bar{v}}{\partial \bar{x}} + \bar{v} \frac{\partial \bar{v}}{\partial \bar{y}} = & -\frac{1}{\rho} \frac{\partial \bar{p}}{\partial \bar{y}} + \nu \bar{\nabla}^2 \bar{v} - \frac{k_0}{\rho} \left[\frac{\partial}{\partial \bar{x}} \left[\left(\bar{u} \frac{\partial}{\partial \bar{x}} + \bar{v} \frac{\partial}{\partial \bar{y}} \right) \left(\frac{\partial \bar{v}}{\partial \bar{x}} + \frac{\partial \bar{u}}{\partial \bar{y}} \right) + \right. \right. \\ & \left. \left. 2 \frac{\partial \bar{u}}{\partial \bar{x}} \frac{\partial \bar{u}}{\partial \bar{y}} + 2 \frac{\partial \bar{v}}{\partial \bar{x}} \frac{\partial \bar{v}}{\partial \bar{y}} \right] + \frac{\partial}{\partial \bar{y}} \left[2\bar{u} \frac{\partial^2 \bar{v}}{\partial \bar{x} \partial \bar{y}} + 2\bar{v} \frac{\partial^2 \bar{v}}{\partial \bar{y}^2} + 4 \left(\frac{\partial \bar{v}}{\partial \bar{y}} \right)^2 + 2 \frac{\partial \bar{u}}{\partial \bar{y}} \left(\frac{\partial \bar{v}}{\partial \bar{x}} + \frac{\partial \bar{u}}{\partial \bar{y}} \right) \right] \right]. \quad (2.10) \end{aligned}$$

In term of the stream function $\bar{\psi}(\bar{x}, \bar{y})$

$$\bar{u} = \frac{\partial \bar{\psi}}{\partial \bar{y}} \quad , \quad \bar{v} = -\frac{\partial \bar{\psi}}{\partial \bar{x}} \quad , \quad (2.11)$$

Eqs. (2.9) and (2.10) takes the form

$$\begin{aligned} \bar{\psi}_{\bar{y}}\bar{\psi}_{\bar{x}\bar{y}} - \bar{\psi}_{\bar{x}}\bar{\psi}_{\bar{y}\bar{y}} &= -\frac{1}{\rho}\bar{p}_{\bar{x}} + \nu[\bar{\psi}_{\bar{x}\bar{x}\bar{y}} + \bar{\psi}_{\bar{y}\bar{y}\bar{y}}] - \frac{k_0}{\rho} \left[13\bar{\psi}_{\bar{x}\bar{y}}\bar{\psi}_{\bar{x}\bar{x}\bar{y}} + \bar{\psi}_{\bar{y}}\bar{\psi}_{\bar{x}\bar{x}\bar{y}} - \bar{\psi}_{\bar{x}}\bar{\psi}_{\bar{x}\bar{x}\bar{y}\bar{y}} \right. \\ &\left. + 4\bar{\psi}_{\bar{x}\bar{x}}\bar{\psi}_{\bar{x}\bar{x}\bar{x}} - 2\bar{\psi}_{\bar{x}\bar{y}\bar{y}}\bar{\psi}_{\bar{x}\bar{x}} - 3\bar{\psi}_{\bar{y}\bar{y}}\bar{\psi}_{\bar{x}\bar{x}\bar{x}} + 3\bar{\psi}_{\bar{y}\bar{y}}\bar{\psi}_{\bar{x}\bar{y}\bar{y}} + \bar{\psi}_{\bar{y}}\bar{\psi}_{\bar{x}\bar{y}\bar{y}\bar{y}} - \bar{\psi}_{\bar{y}\bar{y}\bar{y}\bar{y}}\bar{\psi}_{\bar{x}} + \bar{\psi}_{\bar{y}\bar{y}\bar{y}}\bar{\psi}_{\bar{x}\bar{y}} \right] \quad , \end{aligned} \quad (2.12)$$

$$\begin{aligned} -\bar{\psi}_{\bar{y}}\bar{\psi}_{\bar{x}\bar{x}} + \bar{\psi}_{\bar{x}}\bar{\psi}_{\bar{x}\bar{y}} &= -\frac{1}{\rho}\bar{p}_{\bar{y}} - \nu[\bar{\psi}_{\bar{x}\bar{x}\bar{x}} + \bar{\psi}_{\bar{x}\bar{y}\bar{y}}] - \frac{k_0}{\rho} \left[\bar{\psi}_{\bar{x}\bar{y}}\bar{\psi}_{\bar{x}\bar{x}\bar{x}} - \bar{\psi}_{\bar{y}}\bar{\psi}_{\bar{x}\bar{x}\bar{x}} + 13\bar{\psi}_{\bar{x}\bar{y}}\bar{\psi}_{\bar{x}\bar{y}\bar{y}} - \right. \\ &\left. \bar{\psi}_{\bar{y}}\bar{\psi}_{\bar{x}\bar{x}\bar{y}\bar{y}} + 3\bar{\psi}_{\bar{x}\bar{x}}\bar{\psi}_{\bar{x}\bar{x}\bar{y}} + \bar{\psi}_{\bar{x}}\bar{\psi}_{\bar{x}\bar{x}\bar{y}} + \bar{\psi}_{\bar{x}}\bar{\psi}_{\bar{x}\bar{y}\bar{y}\bar{y}} - 2\bar{\psi}_{\bar{x}\bar{x}\bar{y}}\bar{\psi}_{\bar{y}\bar{y}} - 3\bar{\psi}_{\bar{y}\bar{y}\bar{y}}\bar{\psi}_{\bar{x}\bar{x}} + 4\bar{\psi}_{\bar{y}\bar{y}\bar{y}}\bar{\psi}_{\bar{y}\bar{y}\bar{y}} \right] \quad . \end{aligned} \quad (2.13)$$

For the present flow the appropriate boundary conditions are

$$\bar{\psi} = 0 \quad \frac{\partial \bar{\psi}}{\partial \bar{y}} = c\bar{x} \quad \text{at} \quad \bar{y} = 0, \quad (2.14)$$

$$\bar{\psi} = a\bar{x}\bar{y} + \frac{1}{2}b\bar{y}^2 \quad \text{as} \quad \bar{y} \rightarrow \infty, \quad (2.15)$$

where a , b and c are constants. It is important to mention that boundary condition (2.15) is given by Stuart [16], Tamada [17] and Dorrepaal [18]. Introducing the dimensionless variables

$$x = \bar{x}\sqrt{\frac{c}{\nu}} \quad , \quad y = \bar{y}\sqrt{\frac{c}{\nu}} \quad , \quad \psi = \frac{\bar{\psi}}{\nu} \quad , \quad p = \frac{1}{\rho\nu c}\bar{p}. \quad (2.16)$$

We obtain the transformed system of equations as follows

$$\psi_{xxxx} + \psi_{yyyy} + 2\psi_{xxyy} + \psi_x\psi_{yyy} + \psi_x\psi_{xxy} - \psi_y\psi_{xxx} - \psi_y\psi_{xyy} + We \left[-2\psi_y\psi_{xxyy} \right.$$

$$\left. +2\psi_x\psi_{xxxyy} - \psi_y\psi_{xyyy} + \psi_x\psi_{yyyy} - \psi_y\psi_{xxxx} + \psi_x\psi_{xxxxy} \right] = 0, \quad (2.17)$$

$We = \frac{k_0 c}{\rho \nu}$ is Weissenberg number. The boundary conditions are

$$\psi = 0 \quad \frac{\partial \psi}{\partial y} = x \quad \text{at} \quad y = 0, \quad (2.18)$$

$$\psi = \frac{a}{c}xy + \frac{1}{2}\gamma y^2 \quad \text{as} \quad y \rightarrow \infty, \quad (2.19)$$

where $\gamma = b/c$ is freestream shear stress of fluid.

2.1.1 Transformation from PDE to ODE

Following Tamada [17] and Dorrepaal [18] we assume that

$$\psi(x, y) = xF(y) + G(y), \quad (2.20)$$

where $F(y)$ and $G(y)$ respectively are normal and tangential components of the flow. Substituting (2.20) into Eq. (2.17) and eliminating like powers of x we have

$$-F'(y)F''(y) + F(y)F'''(y) + F^{iv}(y) + We \left[-F'(y)F^{iv}(y) + F(y)F^v(y) \right] = 0, \quad (2.21)$$

$$-G'(y)F''(y) + F(y)G'''(y) + G^{iv}(y) + We \left[-G'(y)F^{iv}(y) + F(y)G^v(y) \right] = 0. \quad (2.22)$$

Integrating (2.21) and (2.22) w.r.t. y

$$F'''(y) + F(y)F''(y) - [F'(y)]^2 + We \left[F(y)F^{iv}(y) - 2F'(y)F'''(y) + [F''(y)]^2 \right] + c_1 = 0, \quad (2.23)$$

$$G'''(y) + F(y)G''(y) - F'(y)G'(y) + We \left[F(y)G^{iv}(y) - F'(y)G'''(y) + F''(y)G''(y) - F'''(y)G'(y) \right] + c_2 = 0. \quad (2.24)$$

Incorporating the free stream conditions, integrating constants are evaluated and resulting equations are given by

$$F''''(y) + F(y)F''(y) - [F'(y)]^2 + \frac{a^2}{c^2} + We \left[F(y)F^{iv}(y) - 2F'(y)F'''(y) + [F''(y)]^2 \right] = 0, \quad (2.25)$$

$$G''''(y) + F(y)G''(y) - F'(y)G'(y) + We \left[F(y)G^{iv}(y) - F'(y)G'''(y) + F''(y)G''(y) - F'''(y)G'(y) \right] = A\gamma, \quad (2.26)$$

where $A = F(\infty) - y_\infty * a/c$ is a constant describing the boundary layer displacement. Now introducing

$$G'(y) = \gamma H(y), \quad (2.27)$$

Eq. (2.26) can be written as

$$H''(y) + F(y)H'(y) - F'(y)H(y) + We \left[F(y)H''''(y) - F'(y)H'''(y) + F''(y)H''(y) - F'''(y)H(y) \right] = A. \quad (2.28)$$

The boundary conditions now take the form

$$F(0) = 0, \quad F'(0) = 1, \quad F'(\infty) = \frac{a}{c}, \quad (2.29)$$

$$G(0) = 0, \quad G'(0) = 0, \quad G''(\infty) = \gamma, \quad (2.30)$$

$$H(0) = 0, \quad H'(\infty) = 1, \quad (2.31)$$

2.1.2 Skin friction

The shear stress for Walters-B fluid is given by [1]

$$\tau^{12} = \mu(\bar{u}_{\bar{y}} + \bar{v}_{\bar{x}}) - k_o \left[\bar{u}(\bar{u}_{\bar{x}\bar{y}} + \bar{v}_{\bar{x}\bar{x}}) + \bar{v}(\bar{u}_{\bar{y}\bar{y}} + \bar{v}_{\bar{x}\bar{y}}) - 2\bar{u}_{\bar{x}}\bar{v}_{\bar{x}} - 2\bar{u}_{\bar{y}}\bar{v}_{\bar{y}} \right], \quad (2.32)$$

in terms of stream function it takes the form

$$\begin{aligned} \tau^{12} = \mu(\bar{\psi}_{\bar{y}\bar{y}} - \bar{\psi}_{\bar{x}\bar{x}}) - k_o \left[\bar{\psi}_{\bar{y}}(\bar{\psi}_{\bar{x}\bar{y}\bar{y}} - \bar{\psi}_{\bar{x}\bar{x}\bar{x}}) - \bar{\psi}_{\bar{x}}(\bar{\psi}_{\bar{y}\bar{y}\bar{y}} - \bar{\psi}_{\bar{x}\bar{x}\bar{y}}) + 2\bar{\psi}_{\bar{x}\bar{y}}\bar{\psi}_{\bar{x}\bar{x}} \right. \\ \left. + 2\bar{\psi}_{\bar{y}\bar{y}}\bar{\psi}_{\bar{x}\bar{y}} \right]. \end{aligned} \quad (2.33)$$

Skin friction at the wall is defined as

$$C_f = \frac{\tau^{12}|_{y=0}}{\rho(c\bar{x})^2}. \quad (2.34)$$

Using (2.16) we have

$$\begin{aligned} Re_x C_f = \left[(\psi_{yy} - \psi_{xx}) - We[\psi_y(\psi_{xyy} - \psi_{xxx}) - \psi_x(\psi_{yyy} - \psi_{xxy}) + 2\psi_{xy}\psi_{xx} \right. \\ \left. + 2\psi_{yy}\psi_{xy} \right]_{y=0}, \end{aligned} \quad (2.35)$$

where $Re_x = \frac{c\bar{x}^2}{\nu}$ is the local Reynolds number. By using (2.20) in (2.35) we have

$$\begin{aligned} Re_x C_f = xF''(0) + G''(0) - We[3xF'(0)F''(0) + F''(0)G'(0) - xF(0)F'''(0) \\ - F(0)G'''(0) + 2F'(0)G''(0)]. \end{aligned} \quad (2.36)$$

By using (2.29) - (2.31) we have

$$Re_x C_f = x(1 - 3We)F''(0) + (1 - 2We)G''(0), \quad (2.37)$$

or

$$Re_x C_f = x(1 - 3We)F''(0) + (1 - 2We)\gamma H'(0). \quad (2.38)$$

2.2 Numerical results and discussion

The hybrid numerical method discussed in detail in section 1.6.1 is implemented in Mathematica to obtain the solution of Eqs. (2.25) and (2.26) subject to boundary conditions (2.29) and (2.30). In order to investigate the influence of the emerging parameters on the velocity profile, graphical results are displayed in Figs. 2.1-2.7. The numerical data of $F''(0)$ for various values of

Weissenberg number We and the stretching parameter a/c are shown in Table 2.1. It is observed that $F''(0)$ decreases for $a/c < 1$. An opposite behavior in the case of $a/c > 1$ is observed for all values of Weissenberg number We . The influence of Viscoelastic and stretching parameters on $H'(0)$ are given in Table 2.2. The table shows that for $a/c < 1$, the values of $H'(0)$ decreases by increasing We and for $a/c > 1$, the value of $H'(0)$ increases by increasing We . An increase in $H'(0)$ is observed by increasing a/c for fixed value of We . Figure 2.1 describes the change in horizontal velocity component $F'(y)$ in response to parameter We when $a/c = 1.2$. As expected, the velocity of the fluid increases by increasing the Weissenberg number We due to increased effective viscosity. It is also interesting to note that the velocity overshoot within the boundary layer is observed for $We \geq 0.2$ and the solution cannot be obtained for $We > 0.3257864$. However, for $a/c < 1$ an opposite trend is presented in Figure 2.2 i.e. the velocity of fluid decreases with an increase in We . The velocity of the fluid undershoots inside the boundary layer for $We \geq 0.2$. Figure 2.3 illustrates the influence of stretching parameter a/c on the velocity profile when $We = 0.1$. It is observed that amplitude of the velocity increases for $a/c > 1$ within the boundary layer and opposite trend is observed for $0 < a/c < 1$. In other words assisting flow has greater values than opposing flow within the boundary layer region. Figure 2.4 describes the effect of Weissenberg We on $H'(y)$ when $a/c = 1.2$. It is found that $H'(y)$ decreases by increasing We . Moreover, one can easily observe that there exist small oscillations in the velocity that vanish at the infinity. An opposite trend is observed in Figure 2.5 for $a/c = 0.5$ i.e. $H'(y)$ increases by increasing We . The graphical presentation of streamline patterns for oblique flow is analyzed in Figure 2.6 and 2.7 for $\gamma = 20$ and $\gamma = -20$, respectively. For $\gamma = 20$ streamlines are inclined leftwards while the streamlines are inclined rightwards for $\gamma = -20$.

Table 2.1: Influence of We and a/c on $F''(0)$.

We	$a/c = 0.1$	$a/c = 0.5$	$a/c = 1.1$	$a/c = 1.2$
0.0	- 0.969372	- 0.667351	0.164288	0.337735
0.05	- 0.997195	- 0.696776	0.176481	0.364668
0.1	- 1.027268	- 0.729988	0.191789	0.399246
0.2	- 1.095630	- 0.810187	0.239295	0.514011
0.3	- 1.177780	- 0.914228	0.352166	0.911348

Table 2.2: Influence of We and a/c on $H'(0)$.

We	$a/c = 0.1$	$a/c = 0.5$	$a/c = 1.1$	$a/c = 1.2$
0.0	0.226050	0.786921	1.006500	1.049188
0.05	0.211284	0.767119	1.029299	1.055435
0.1	0.189237	0.749586	1.033345	1.063717
0.2	0.147573	0.707326	1.045012	1.080598
0.3	0.110617	0.648268	1.050152	1.085944

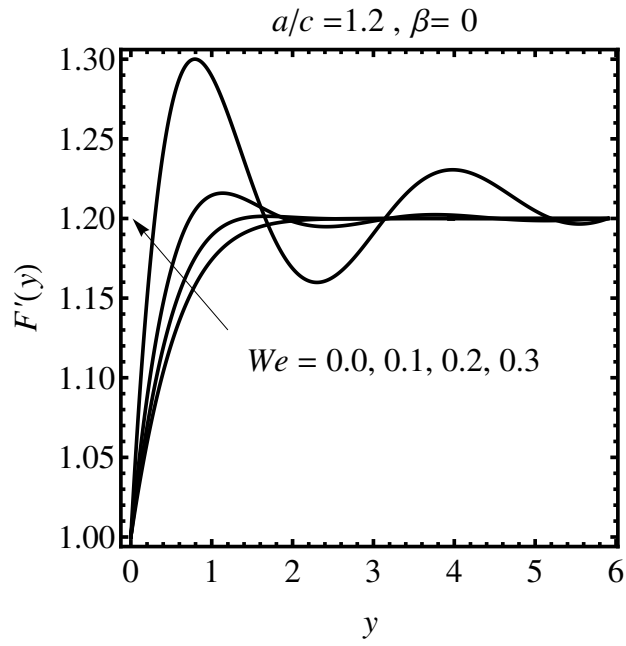


Figure 2.1: Effects of We on $F'(y)$ when $a/c = 1.2$.

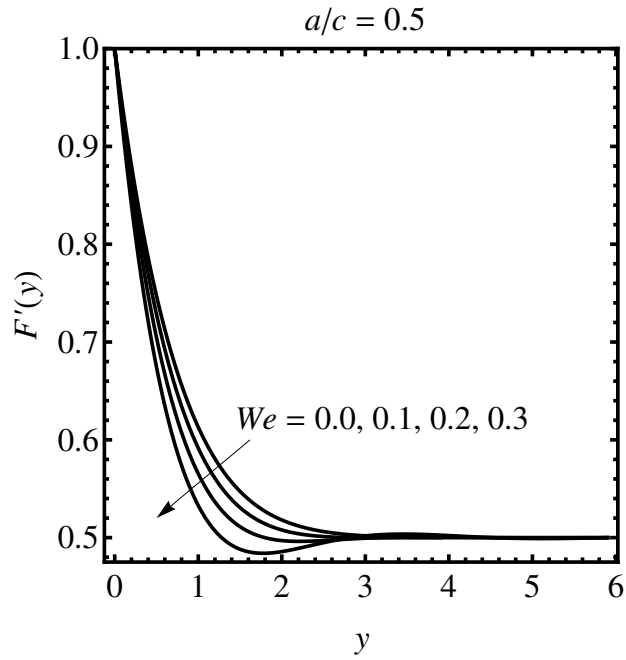


Figure 2.2: Effects of We on $F'(y)$ when $a/c = 0.5$.

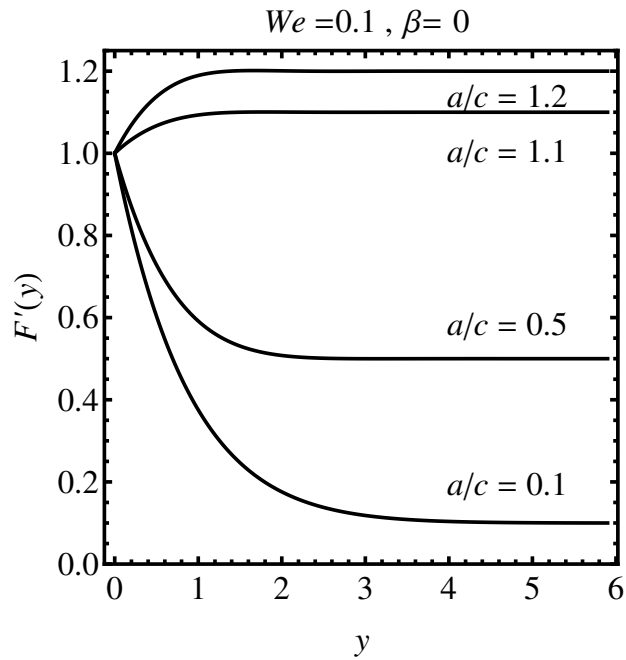


Figure 2.3: Effects of parameter a/c on $F'(y)$ when $We = 0.1$.

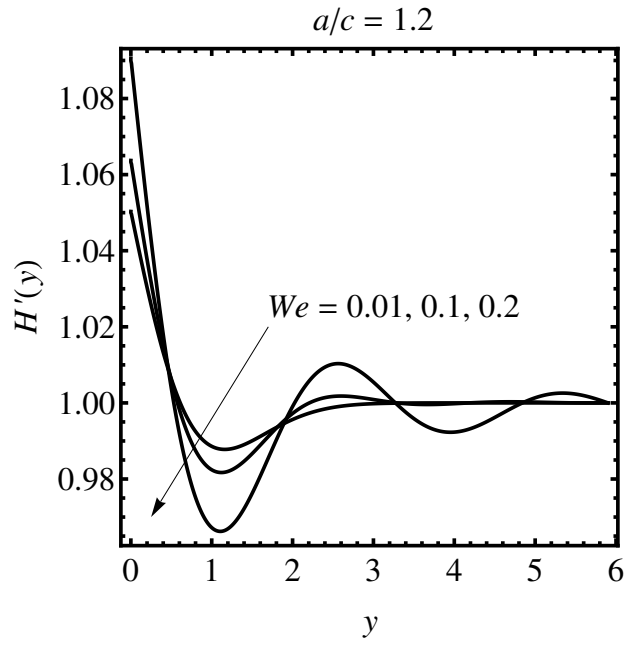


Figure 2.4: Effects of We on $H'(y)$ when $a/c = 1.2$.

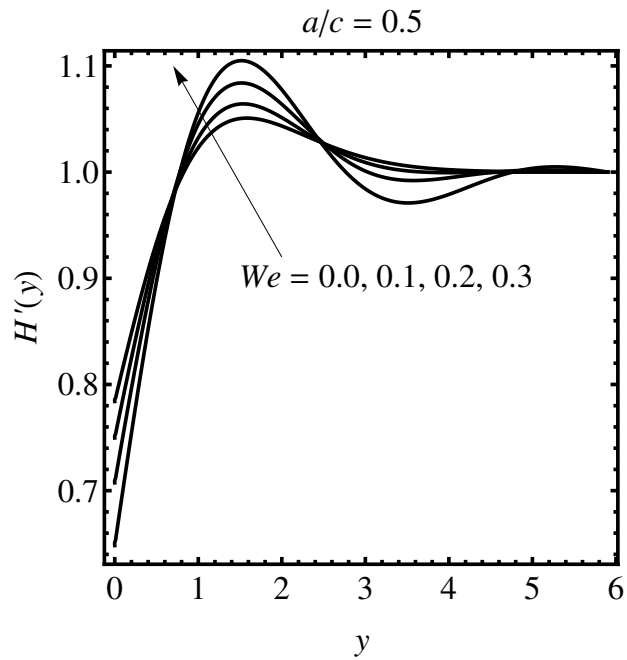


Figure 2.5: Effects of We on $H'(y)$ when $a/c = 0.5$.

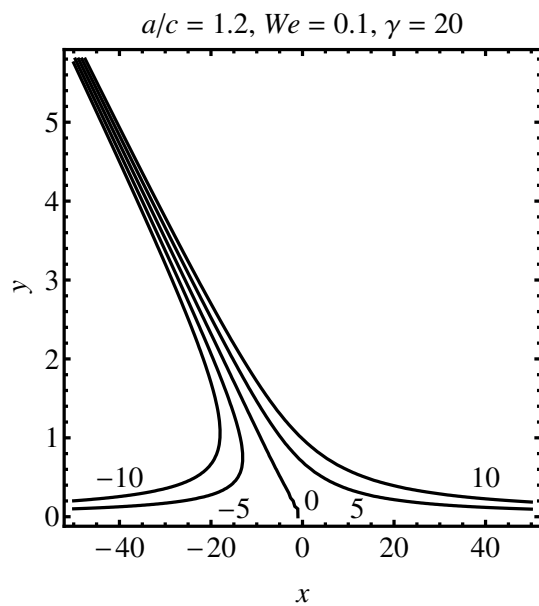


Figure 2.6: Streamline patterns for oblique flow when $a/c = 1.2, We = 0.1$ and $\gamma = 20$.

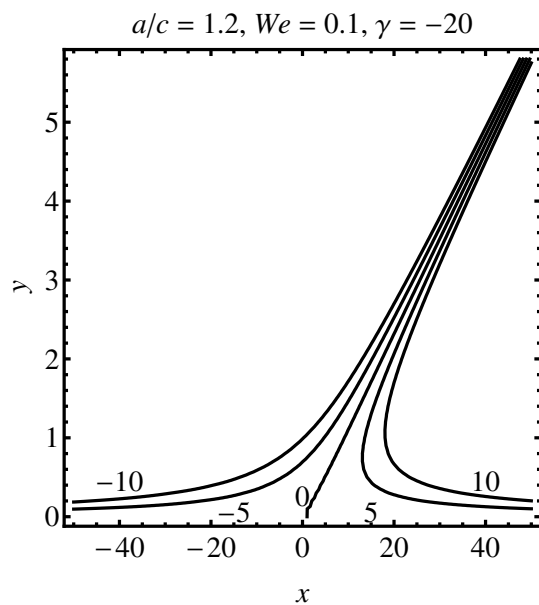


Figure 2.7: Streamline patterns for oblique flow when $a/c = 1.2, We = 0.1$ and $\gamma = -20$.

Chapter 3

Slip and radiation effects for two-dimensional oblique stagnation point flow towards a stretching surface in a viscoelastic fluid by using hybrid method

The aim of this chapter is to extend the analysis carried out in previous chapter for the slip and radiation effects. A numerical solution is obtained by using the hybrid numerical method [3] and shooting method [15]. Numerical and graphical results for different parameters are presented and discussed in detail.

3.1 Mathematical formulation

3.1.1 Slip condition

The flow analysis here is governed by the same set of equations (2.25), (2.26) and (2.28) described in detail in previous chapter. However, the no-slip condition is replaced with the Navier [12] slip condition which states that the velocity at the surface proportionally relates to the shear stress at the surface, mathematically for the present flow situation we can write

$$\bar{u} = c\bar{x} + \frac{l}{\mu}\tau^{12}|_{\bar{y}=0}, \quad (3.1)$$

where l is the slip length. In terms of dimensionless variables (2.16) we get

$$\psi_y = x + \beta \left((\psi_{yy} - \psi_{xx}) - We[\psi_y(\psi_{xyy} - \psi_{xxx}) - \psi_x(\psi_{yyy} - \psi_{xxy}) + 2\psi_{xy}\psi_{xx} + 2\psi_{yy}\psi_{xy}] \right)_{y=0}, \quad (3.2)$$

where $\beta = l\sqrt{\frac{\epsilon}{\nu}}$ is the slip parameter. Substituting Eq. (2.51) in (3.2) and eliminating like powers of x we have

$$F'(0) = 1 + \beta[F''(0) - 3WeF'(0)F''(0)], \quad (3.3)$$

or

$$F'(0) = \frac{1 + \beta F''(0)}{1 + 3\beta We F''(0)}. \quad (3.4)$$

$$G'(0) = \beta G''(0) - \beta We[F''(0)G'(0) + 2F'(0)G''(0)], \quad (3.5)$$

or

$$G'(0) = \frac{\beta G''(0)}{1 + \beta We F''(0)} \left[1 - 2We \left(\frac{1 + \beta F''(0)}{1 + 3\beta We F''(0)} \right) \right]. \quad (3.6)$$

$$F(0) = 0, \quad F'(0) = \frac{1 + \beta F''(0)}{1 + 3\beta We F''(0)}, \quad F'(\infty) = \frac{a}{c}, \quad (3.7)$$

$$G(0) = 0, \quad G'(0) = \frac{\beta G''(0)}{1 + \beta We F''(0)} \left[1 - 2We \left(\frac{1 + \beta F''(0)}{1 + 3\beta We F''(0)} \right) \right],$$

$$G''(\infty) = \gamma. \quad (3.8)$$

3.1.2 Energy equation

Equation that governs heat transfer with radiation effects and heat source/sink in absence of viscous dissipation is given by

$$\bar{u} \frac{\partial T}{\partial \bar{x}} + \bar{v} \frac{\partial T}{\partial \bar{y}} = \frac{k}{\rho c_p} \frac{\partial^2 T}{\partial \bar{y}^2} - \frac{1}{\rho c_p} \frac{\partial q_r}{\partial \bar{y}} + \frac{Q}{\rho c_p} (T - T_\infty), \quad (3.9)$$

with

$$T = T_w \quad \text{at} \quad \bar{y} = 0, \quad T \rightarrow T_\infty \quad \text{at} \quad \bar{y} \rightarrow \infty, \quad (3.10)$$

where T , T_w and T_∞ respectively are the fluid temperatures inside the boundary layer, at the wall and far away from stretching sheet. k , c_p , q_r and Q respectively are thermal conductivity, specific heat constant, radiative heat flux and heat source/sink. $Q > 0$ represents the heat source and $Q < 0$ represents the heat sink. Using Rossland approximation

$$q_r = \frac{-4\sigma^*}{3k^*} \frac{\partial T^4}{\partial \bar{y}}, \quad (3.11)$$

in above Eq. σ^* and k^* respectively are the Stefan Boltzmann constant and the mean absorption coefficient. Taylor series of T^4 is given by

$$T^4 = 4T_\infty^3 T - 3T_\infty^4. \quad (3.12)$$

Let $\alpha = k/\rho c_p$ and using (3.11) and (3.12) in (3.9) we have

$$\bar{u} \frac{\partial T}{\partial \bar{x}} + v \frac{\partial T}{\partial \bar{y}} = \alpha \frac{\partial^2 T}{\partial \bar{y}^2} + \frac{1}{\rho c_p} \frac{16\sigma^* T_\infty^3}{3k^*} \frac{\partial^2 T}{\partial \bar{y}^2} + \frac{Q}{\rho c_p} (T - T_\infty), \quad (3.13)$$

$$\bar{u} \frac{\partial T}{\partial \bar{x}} + v \frac{\partial T}{\partial \bar{y}} = \left(\alpha + \frac{1}{\rho c_p} \frac{16\sigma^* T_\infty^3}{3k^*} \right) \frac{\partial^2 T}{\partial \bar{y}^2} + \frac{Q}{\rho c_p} (T - T_\infty). \quad (3.14)$$

In term of dimensionless variables it can be written as

$$c\psi_y \frac{\partial T}{\partial x} - c\psi_x \frac{\partial T}{\partial y} = \left(\alpha + \frac{1}{\rho c_p} \frac{16\sigma^* T_\infty^3}{3k^*} \right) \frac{\partial^2 T}{\partial y^2} \frac{c}{\nu} + \frac{Q}{\rho c_p} (T - T_\infty). \quad (3.15)$$

Introducing the transformation

$$T = T_\infty + \theta(y)(T_w - T_\infty). \quad (3.16)$$

Using (2.20) and (3.16) into (3.15) we have

$$-F(y)\theta'(y)(T_w - T_\infty) = \left(\alpha + \frac{1}{\rho c_p} \frac{16\sigma^* T_\infty^3}{3k^*} \right) \frac{1}{\nu} \theta''(y)(T_w - T_\infty) + \frac{Q}{c\rho c_p} (T - T_\infty), \quad (3.17)$$

$$-\frac{\mu c_p}{k} F(y)\theta'(y) = \theta''(y) + \frac{16\sigma^* T_\infty^3}{3k^* k} \theta''(y) + \frac{\mu c_p}{k} \frac{Q}{c\rho c_p} \theta(y), \quad (3.18)$$

$$-Pr F(y) \theta'(y) = \theta''(y) + Nr \theta''(y) + Pr \lambda \theta(y), \quad (3.19)$$

where $Pr = \frac{\mu c_p}{k}$, $Nr = \frac{16\sigma^* T_\infty^3}{3k^* k}$ and $\lambda = \frac{Q}{c\rho c_p}$ are Prandtl number, radiation parameter and the dimensionless heat source or sink parameter respectively.

$$(1 + Nr) \theta''(y) + Pr F(y) \theta'(y) + Pr \lambda \theta(y) = 0, \quad (3.20)$$

$$\theta''(y) + \frac{Pr}{1 + Nr} F(y) \theta'(y) + \frac{Pr}{1 + Nr} \lambda \theta(y) = 0, \quad (3.21)$$

$$\theta''(y) + Pr_{eff} F(y) \theta'(y) + Pr_{eff} \lambda \theta(y) = 0, \quad (3.22)$$

where $Pr_{eff} = \frac{Pr}{1 + Nr}$ is the effective Prandtl number [20]. The Transformed boundary conditions are

$$\theta(0) = 1 \quad \theta(\infty) = 0. \quad (3.23)$$

The physical quantity of interest is the local Nusselt number defined as

$$Nu_x = \frac{\bar{x} q_w}{k(T_w - T_\infty)}, \quad (3.24)$$

where q_w is local heat flux defined by

$$q_w = -k \left(1 + \frac{16\sigma^* T_\infty^3}{3k^* k} \right) \left(\frac{\partial T}{\partial \bar{y}} \right)_{\bar{y}=0}. \quad (3.25)$$

Using (2.16) and (3.16), then simplifying we have

$$Re_x^{-1/2} Nu_x^* = -\theta'(0), \quad (3.26)$$

where $Nu_x^* = Nu_x / (1 + Nr)$ is the effective local Nusselt number.

3.2 Numerical results and discussion

Slip and radiation effects for oblique stagnation-point flow of Walters-B fluid over a stretching surface are analyzed using a hybrid numerical method. The numerical and graphical results are presented in this section. Table 3.1 presents

the influence of Weissenberg number We , stretching parameter a/c and the slip parameter β on $F''(0)$. It is clear from the table that $F''(0)$ increases by increasing the Weissenberg number and stretching parameter while decreases by increasing the slip β . The influences of Weissenberg number We , stretching parameter a/c , slip parameter β , effective Prandtl number Pr_{eff} and heat source/sink parameter λ on the effective local Nusselt number $-\theta(0)$ are discussed in Table 3.2. It is found that the value of effective local Nusselt number decreases by increasing heat source/sink parameter while other parameters show opposite effects. Figures 3.1 depicts the effect of Weissenberg number We on the velocity $F'(y)$ when $a/c = 1.2$ and $\beta = 1$. An increase in Weissenberg number We enhances the velocity. Moreover, the presence of slip alters the velocity of the fluid. Figure 3.2 exhibits the nature of $F'(y)$ against We for $0 < a/c < 1$. The fluid velocity and the momentum boundary layer thickness reduces with increasing We . Effects of stretching parameter a/c on $F'(y)$ are shown in Figure 3.3. The velocity profile increases for $a/c > 1$ while decreases in the case $a/c < 1$. Figures 3.4 and 3.5 are plotted to see the variation of velocity profile against slip parameter β for $a/c > 1$ and $0 < a/c < 1$ respectively. We noted that the velocity increases by increasing the slip parameter β in case of $a/c > 1$ while in case of $0 < a/c < 1$, the observations are quite opposite i.e. the velocity decreases by increasing β . The variation of $H'(0)$ for changing Weissenberg number We in the presence of the slip is shown in Figure 3.6. It is evident that the velocity is larger when We increases. It is also interesting to observe that the shear velocity overshoots when $We > 0.1$. The graphical representation of effects of Weissenberg number We on temperature is discussed in Figure 3.7. The temperature profile and thermal boundary layer thickness increases by increasing We . Figure 3.8 analyze the effects of stretching parameter a/c on the temperature profiles. The temperature profile and the thermal boundary layer thickness reduce with increase of a/c . The temperature profile for various values of slip parameter β is discussed in Figure 3.9. We observe that temperature increases for higher values of slip parameter β . Figure 3.10 presents the effects of effective Prandtl number Pr_{eff} on temperature profile. This figure shows that temperature is a decreasing function of the effective Prandtl number Pr_{eff} . In fact, the thermal diffusivity is decreased for large effective Prandtl number which corresponds to decrease in the temperature of the fluid. In order to see the response of temperature for various values of heat source/sink, Figure 3.11 is interpreted. With increase of heat source, the rate of heat transfer from sheet to source becomes larger

which increases the temperature. However, the temperature decreases in case of heat sink. The graphical analysis of stream function for changing We are shown in Figure 3.12. The solid lines correspond to $We = 0.1$ while dashed lines represent the stream lines for $We = 0.3$. In this case stagnation-point moves rightwards by increasing We . Streamlines pattern for various values of parameters β are shown in the Fig. 3.13. An increment in the slip parameter β moves stagnation-point leftwards. Streamlines for changing stretching parameter a/c are shown in Fig. 3.14. Stagnation-point moves rightwards by increasing a/c .

Table 3.1: Influence of $F''(0)$ for various values of We , a/c and β .

We	a/c	β	$F''(0)$
0.1	1.2	0.5	0.241033
0.0			0.184738
0.1			0.241033
0.2			0.355157
0.3			0.771702
	0.1		-0.647023
	0.5		-0.453582
	1.1		0.116202
	1.2		0.241033
		0.0	0.399251
		0.5	0.241033
		1	0.173351
		2	0.111267
		5	0.053748

Table 3.2: Influence of $-\theta'(0)$ for various values of We , a/c , β , Pr_{eff} and λ .

We	a/c	β	Pr_{eff}	λ	$-\theta'(0)$
0.1	1.2	0.5	2	0.2	1.050671
0.0					1.050422
0.1					1.050671
0.2					1.053434
0.3					1.075769
	0.1				0.537222
	0.5				0.725719
	1.1				1.007645
	1.2				1.050671
		0.0			1.025031
		0.5			1.050671
		1			1.061183
		2			1.070603
		5			1.079149
			0.5		0.549541
			1		0.749232
			2		1.050671
			5		1.647305
				-1	1.815617
				-0.5	1.533860
				0.0	1.202865
				0.5	0.791830
				1	0.228288

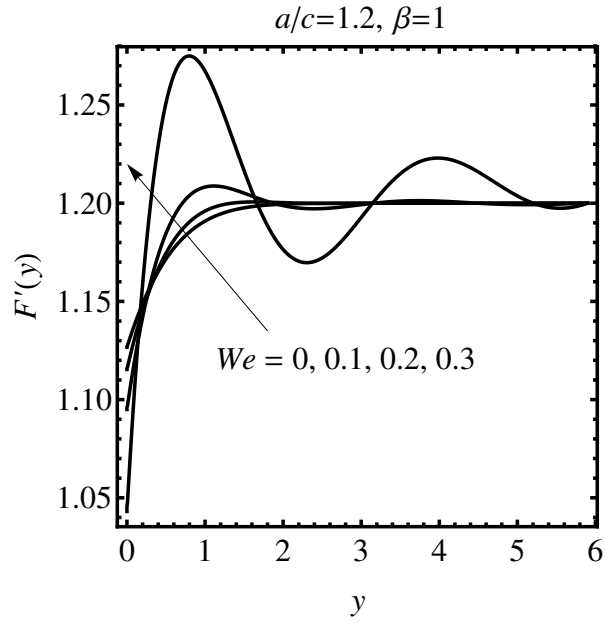


Figure 3.1: Effects of We on $F'(y)$ when $a/c = 1.2$ in the case of slip.

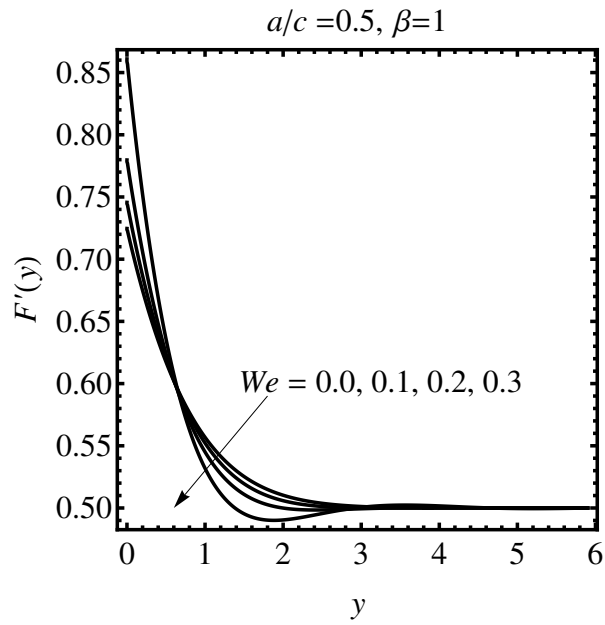


Figure 3.2: Effects of We on $F'(y)$ when $a/c = 0.5$ in the case of slip.

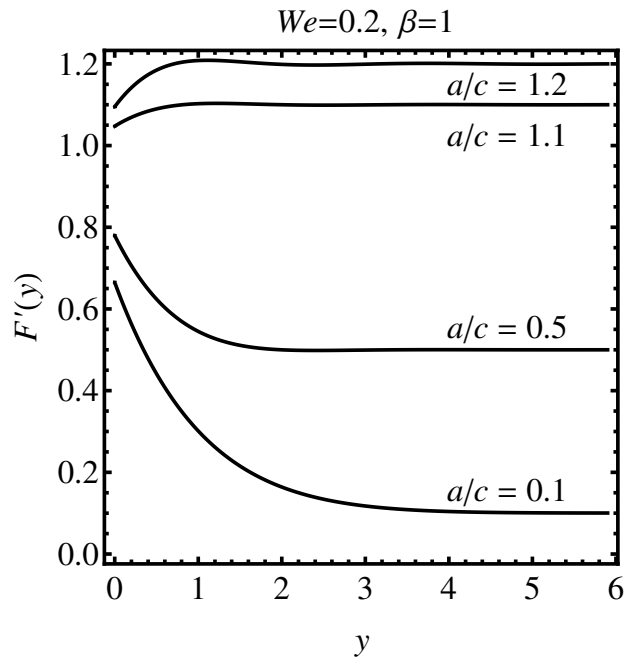


Figure 3.3: Effects of a/c on $F'(y)$ in the case of slip.

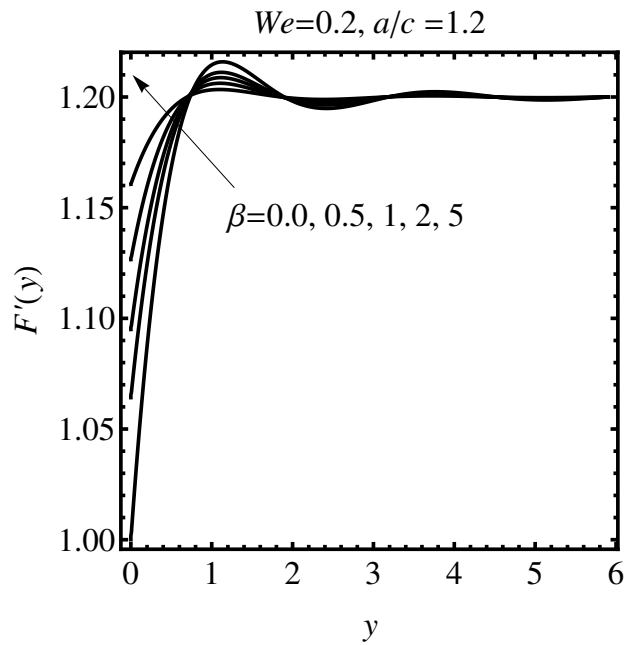


Figure 3.4: Effects of β on $F'(y)$ when $a/c = 1.2$.

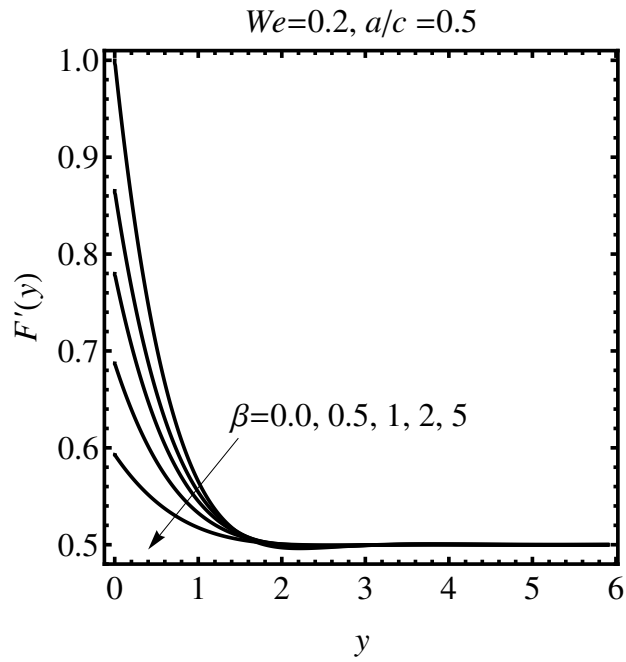


Figure 3.5: Effects of β on $F'(y)$ when $a/c = 0.5$.

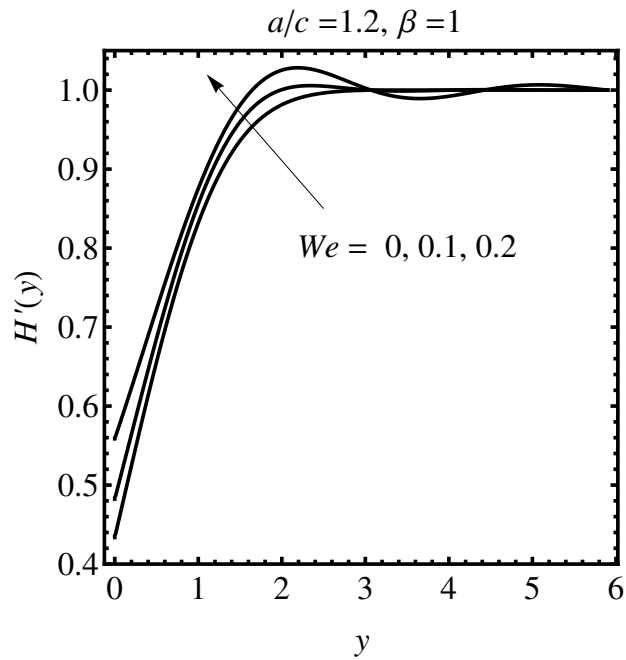


Figure 3.6: Effects of We on $H'(y)$ in the case of slip.

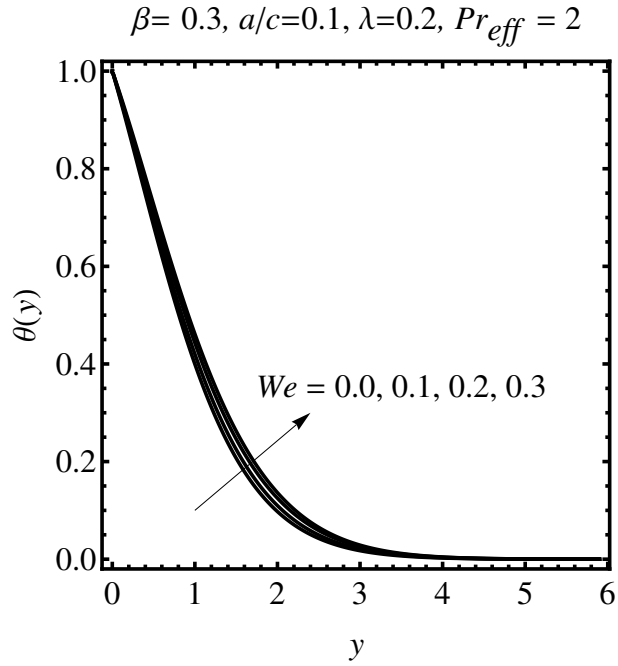


Figure 3.7: Effects of We on temperature $\theta(y)$.

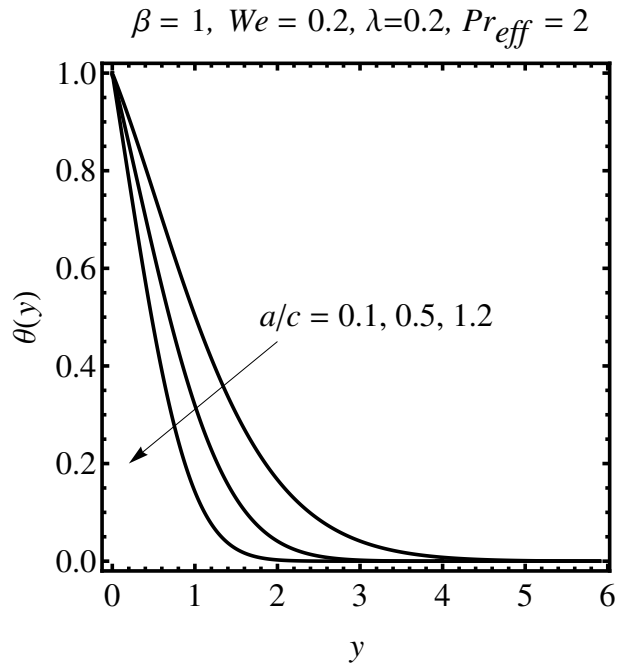


Figure 3.8: Effects of a/c on temperature $\theta(y)$.

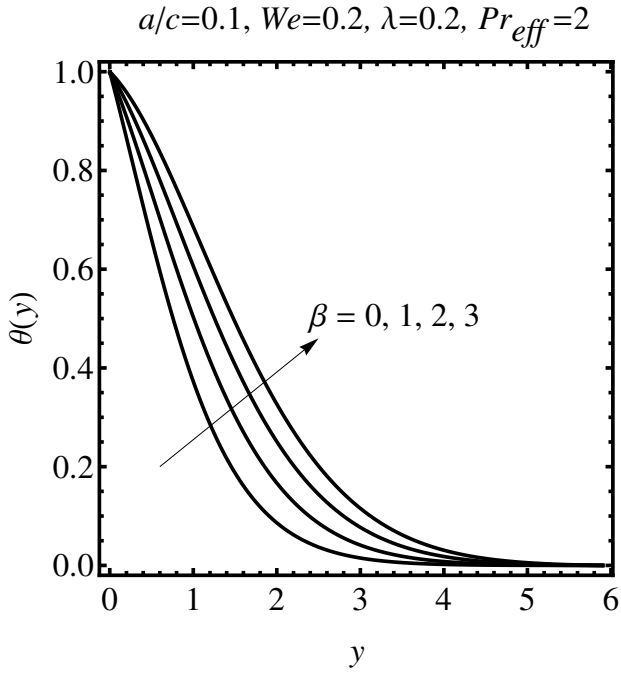


Figure 3.9: Effects of β on temperature $\theta(y)$.

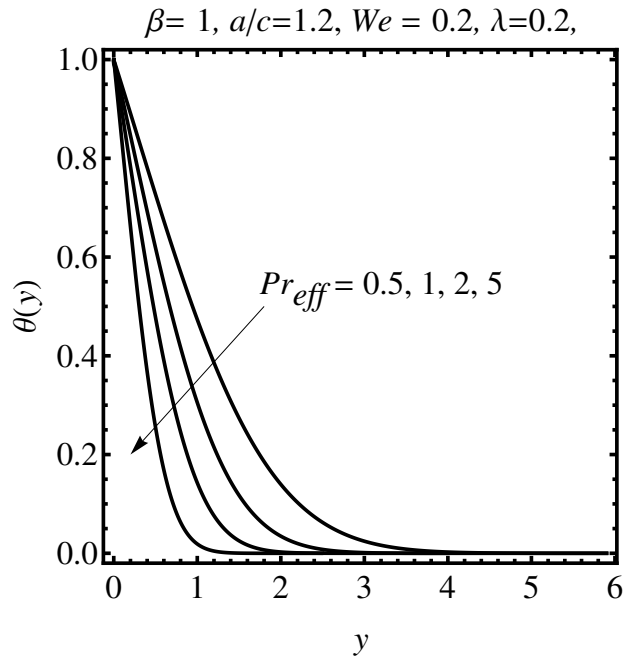


Figure 3.10: Effects of Pr_{eff} on temperature $\theta(y)$.

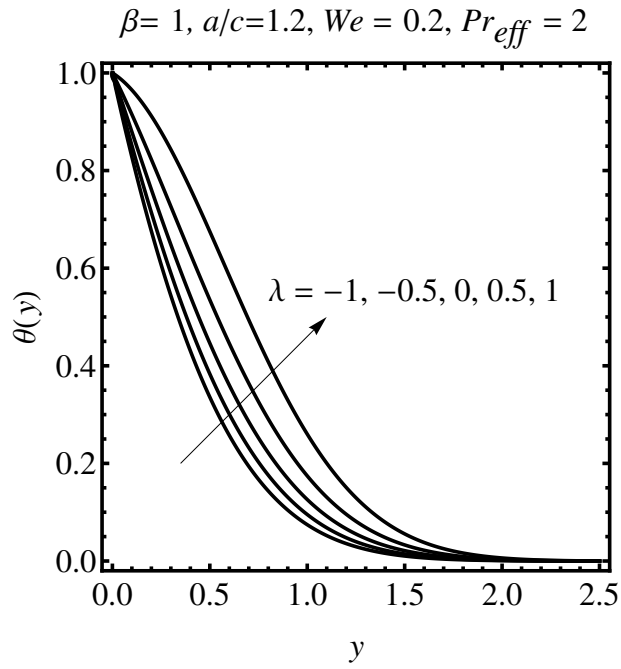


Figure 3.11: Effects of λ on temperature $\theta(y)$.

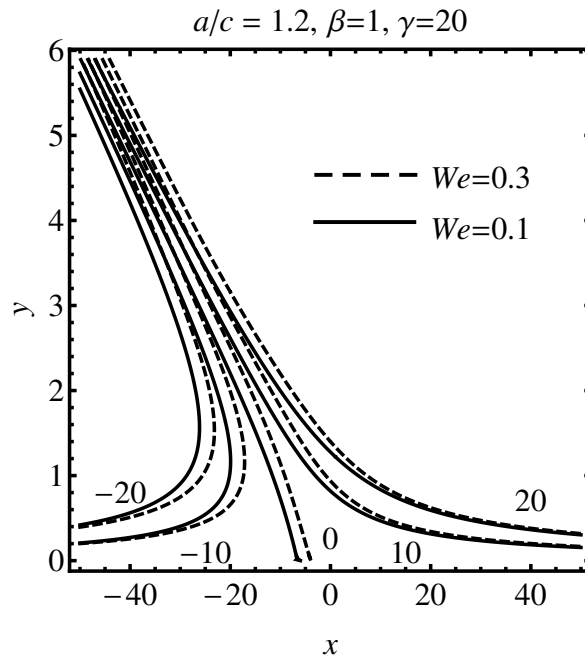


Figure 3.12: Streamlines pattern for various values of We in the case of slip.

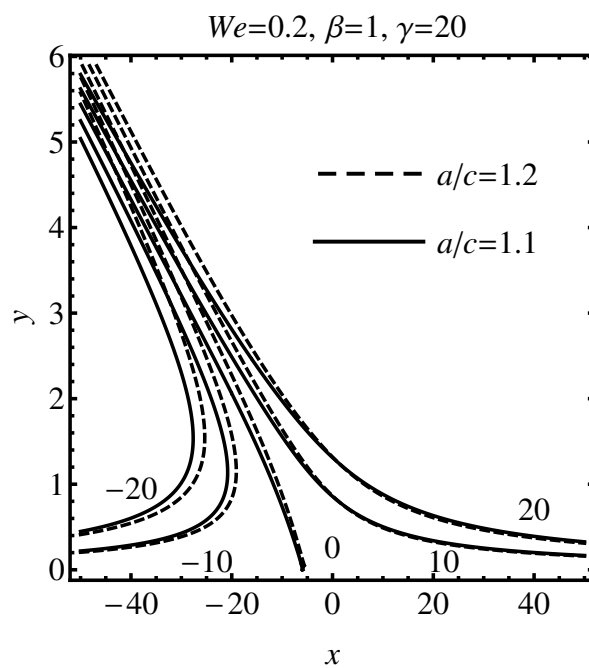


Figure 3.13: Streamlines pattern for various values of a/c in the case of slip.

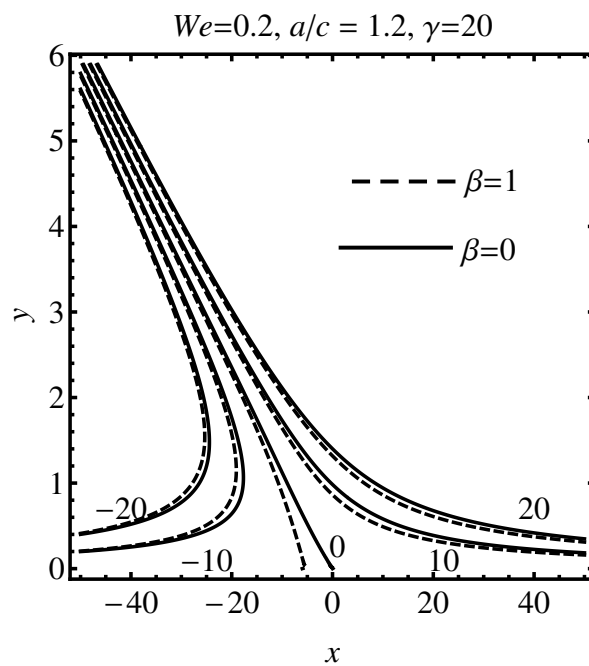


Figure 3.14: streamlines pattern for various values of β in the case of slip.

Chapter 4

A Legendre wavelet spectral collocation method for two-dimensional oblique stagnation point flow of Walters-B fluid with heat transfer

In this chapter the details of slip and radiation effects in two-dimensional oblique stagnation-point flow due to a stretching surface in Walters-B fluid are discussed. The governing transformed ordinary differential equations discussed in chapter 3 are solved numerically by using Legendre wavelet spectral collocation method (LWSM) [14] explained in section (1.6.3) in combination with the shooting method [15] explained in section (1.6.1). Numerical and graphical results are presented and discussed for various values of emerging parameters.

4.1 Solution by the Legendre wavelet spectral collocation method

Consider the boundary value problem

$$F''' + FF'' - F'^2 + \frac{a^2}{c^2} + We \left[FF^{iv} - 2F'F''' + F''^2 \right] = 0, \quad (4.1)$$

$$F(0) = 0, \quad F'(0) = \frac{1 + \beta F''(0)}{1 + 3\beta We F''(0)}, \quad F'(\infty) = \frac{a}{c}. \quad (4.2)$$

First boundary value problem is converted into initial value problem by using shooting method assuming

$$F''(0) = s, \quad (4.3)$$

Differentiating (4.1) - (4.3) w.r.t. s we get

$$Z''' + ZF'' + FZ'' - 2F'Z' + We \left[ZF^{iv} + FZ^{iv} - 2Z'F''' - 2F'Z''' + 2F''Z'' \right] = 0, \quad (4.4)$$

$$Z(0) = 0, \quad Z'(0) = \frac{\beta(1 - 3We)}{(1 + 3\beta We F''(0))^2}, \quad Z''(0) = 1. \quad (4.5)$$

The approximate solution of the resulting initial value problem (4.1)-(4.5), we divide the domain $0 < y < T$ into subintervals given by

$$\left[\frac{n-1}{2^{k-1}}, \quad \frac{n}{2^{k-1}} \right), \quad (4.6)$$

for $n = 1, \dots, 2^{k-1}T$. The Legendre wavelet interpolation approximation to the functions $F(y)$ and $Z(y)$ on the n th subinterval by following Eq. (1.72) is given by

$$F(y) \simeq \sum_{n=1}^{2^{k-1}T} F_n(y) = \sum_{n=1}^{2^{k-1}T} \sum_{j=0}^{M-1} I_{nj}(y) F(y_{nj}), \quad (4.7)$$

$$Z(y) \simeq \sum_{n=1}^{2^{k-1}T} Z_n(y) = \sum_{n=1}^{2^{k-1}T} \sum_{j=0}^{M-1} I_{nj}(y) Z(y_{nj}), \quad (4.8)$$

and

$$F^m(y) \simeq \sum_{n=1}^{2^{k-1}T} F_n^m(y) = \sum_{n=1}^{2^{k-1}T} \sum_{j=0}^{M-1} I_{nj}^m(y) F(y_{nj}), \quad (4.9)$$

$$Z^m(y) \simeq \sum_{n=1}^{2^{k-1}T} Z_n^m(y) = \sum_{n=1}^{2^{k-1}T} \sum_{j=0}^{M-1} I_{nj}^m(y) F(y_{nj}). \quad (4.10)$$

Applying the points $y_{nj} \mid n = 1, \dots, 2^{k-1}T, j = 3, \dots, M-1$ into Eqs. (4.1) and (4.4)

$$F_n''' + F_n F_n'' - F_n'^2 + \frac{a^2}{c^2} + We \left[F_n F_n^{iv} - 2F_n' F_n''' + F_n''^2 \right] = 0, \quad (4.11)$$

$$Z_n''' + Z_n F_n'' + F_n Z_n'' - 2F_n' Z_n' + We \left[Z_n F_n^{iv} + F_n Z_n^{iv} - 2Z_n' F_n''' \right]$$

$$-2F'_n Z_n''' + 2F''_n Z_n'' = 0, \quad (4.12)$$

with the initial conditions in the first subinterval are

$$F_1(0) = 0, \quad F'_1(0) = \frac{1 + \beta F''_1(0)}{1 + 3\beta We F''_1(0)}, \quad F''_1(0) = s, \quad (4.13)$$

$$Z_1(0) = 0, \quad Z'_1(0) = \frac{\beta(1 - 3We)}{(1 + 3\beta We F''_1(0))^2}, \quad Z''_1(0) = 1. \quad (4.14)$$

We set $n = 1$ and choose an approximate value for s . Then the initial value problem (4.11) and (4.12) with the initial conditions (4.13) and (4.14) are solved in the first subinterval $[0, 1/2^{k-1})$. Initial conditions for the second subinterval are evaluated from the first subinterval and solution for second subinterval is obtained. The process continues till the last subinterval. The values of s are modified with the zero finding algorithm defined as

$$s^{n+1} = s^n - \frac{F'(\infty, s^n) - a/c}{Z'(\infty, s^n)}. \quad (4.15)$$

4.2 Numerical results and discussion

The boundary layer stagnation point flow problem discussed in chapter 3 using a hybrid numerical method is revisited and solved by an iterative Legendre wavelet spectral collocation method in combination with the shooting method in this chapter. The anomalies associated with the velocity profile for large Weissenberg number have been addressed. The overshoot/undershoot in the velocity profiles for large Weissenberg number is controlled through the implementation of the proposed method. In tables 4.1 and 4.2 the numerical values of the missing boundary conditions are provided. Table 4.3 is presented to show the influence of We , a/c and slip parameter β on the numerical values of $F''(0)$. Numerical values of $\theta'(0)$ for different values of emerging parameters are given in table 4.4. It is evident from the table 4.4 that heat transfer rate increases with parameters We , a/c , β and Pr_{eff} and decreases with λ . Figure 4.1 is displayed to show the influence of We on the velocity profile $F'(y)$. This figure depicts that no overshoot in velocity is observed. Furthermore, the results are also evaluated for $We > 0.3257864$. In Figure 4.2 in the case of $a/c < 1$ no undershoot is observed in the velocity profile for large We as predicted in previous studies in the case of no-slip. Figures 4.3 and 4.4 are presented to show the influence of We on $H'(y)$. The oscillations observed in

Figures 2.4 and 2.5 are controlled in the free stream. Effects of Weissenberg number in presence of slip are discussed in Figures 4.5 and 4.6. In the presence of slip overshoot/undershoot in the velocity is controlled. The slip effects on the velocity profile $F'(y)$ are shown in the Figures 4.7 and 4.8. These figures elucidate that the large values of slip dominates the effects of free stream velocity and for the full slip case there will be no variation in the velocity. The effects of We on $H'(y)$ in presence of slip are discussed in Figure 4.9. No oscillation is observed in presence of slip. Figures 4.10-4.17 are made to compare the two numerical solution discussed in Chapter 3 and 4. These figures clearly illustrate that our numerical scheme controls the overshoot/undershoot in the velocity. The residual errors for different We are presented in Figures 4.18-4.20. It is evident that our results are within an accuracy of 10^{-6} .

Table 4.1: Influence of $F''(0)$ for different values of We and a/c .

We	$a/c = 0.1$	$a/c = 0.5$	$a/c = 1.1$	$a/c = 1.2$
0.0	-0.969478	-0.667284	0.164293	0.337744
0.05	-0.997033	-0.696570	0.176353	0.364366
0.1	-1.026342	-0.728904	0.191053	0.397446
0.2	-1.091446	-0.804906	0.233221	0.496825
0.3	-1.168468	-0.901446	0.312576	0.708356
0.35	-1.213554	-0.960658	0.390439	0.965354

Table 4.2: Influence of $H'(0)$ for different values of We and a/c .

We	$a/c = 0.1$	$a/c = 0.5$	$a/c = 1.1$	$a/c = 1.2$
0.0	0.235161	0.782688	1.02620	1.04918
0.05	0.211202	0.766367	1.02995	1.05658
0.1	0.185209	0.746639	1.03469	1.06012
0.2	0.129112	0.740619	1.06060	1.12485
0.3	0.066623	0.681716	1.10580	1.23018
0.35	0.039690	0.562384	1.13379	1.28813

Table 4.3: Influence of $F''(0)$ for various values of We , a/c and β .

We	a/c	β	$F''(0)$
0.1	1.2	0.5	0.240334
0.0			0.184739
0.1			0.240334
0.2			0.346492
0.3			0.626779
0.35			1.043361
	0.1		-0.646816
	0.5		-0.453255
	1.1		0.115923
	1.2		0.240334
		0.0	0.397442
		0.5	0.240334
		1	0.172973
		2	0.111109
		5	0.053710

Table 4.4: Influence of $-\theta'(0)$ for various values of We , a/c , β , Pr_{eff} and λ .

We	a/c	β	Pr_{eff}	λ	$-\theta'(0)$
0.1	1.2	0.5	2	0.2	1.050579
0.0					1.050406
0.1					1.050579
0.2					1.109237
0.3					1.624092
0.35					2.116743
	0.1				0.502232
	0.5				0.723799
	1.1				1.007576
	1.2				1.050579
		0.0			1.024890
		0.5			1.050579
		1			1.060978
		2			1.070634
		5			1.080384
			0.5		0.576741
			1		0.755698
			2		1.050579
			5		1.646832
				-1	1.815485
				-0.5	1.533712
				0.0	1.202735
				0.5	0.791887
				1	0.229412

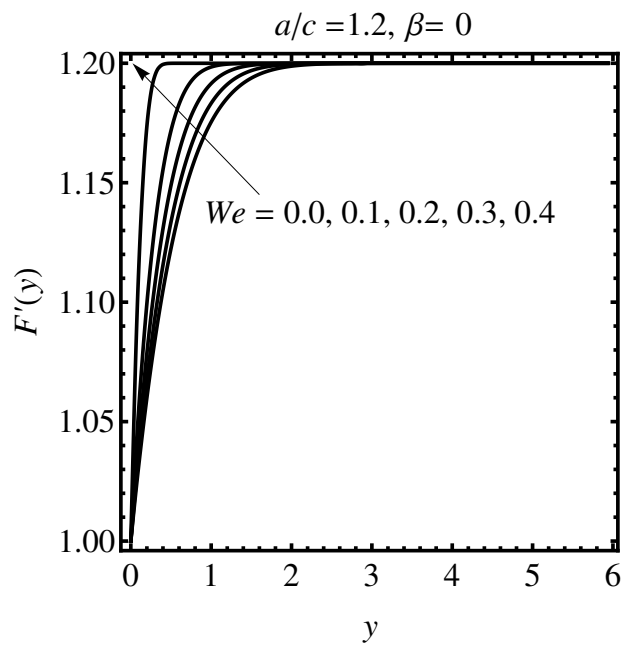


Figure 4.1: Effects of We on $F'(y)$ when $a/c = 1.2$.

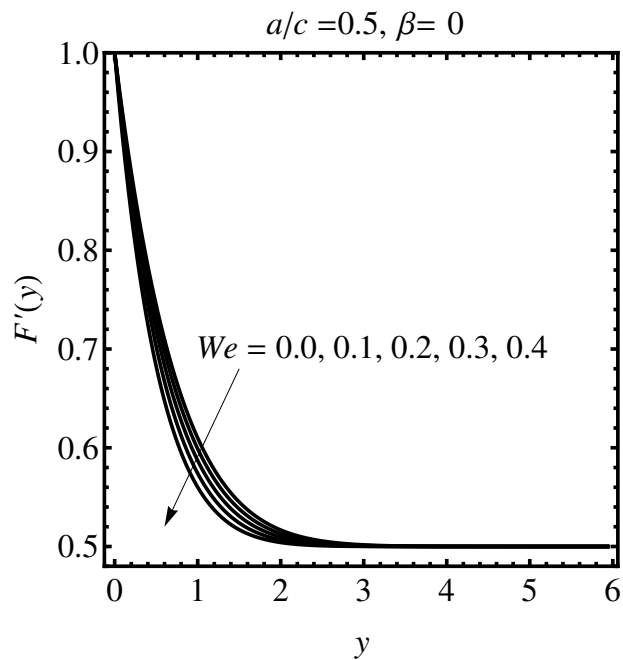


Figure 4.2: Effects of We on $F'(y)$ when $a/c = 0.5$.

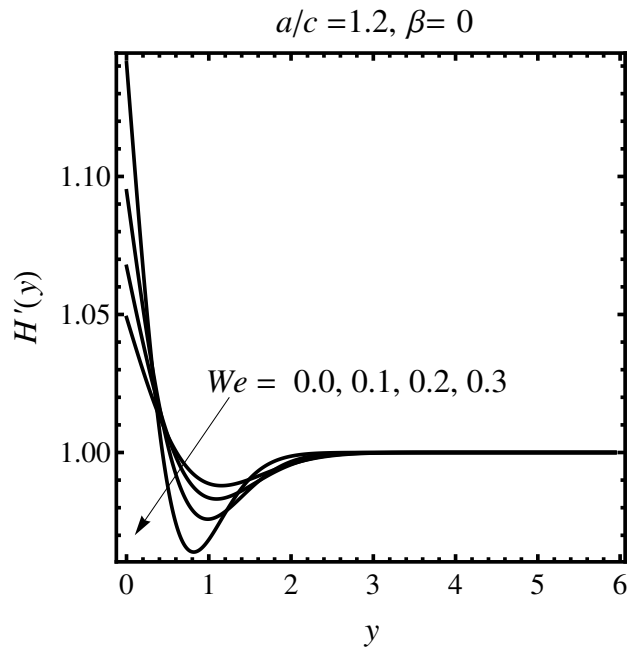


Figure 4.3: Effects of We on $H'(y)$ when $a/c = 1.2$.

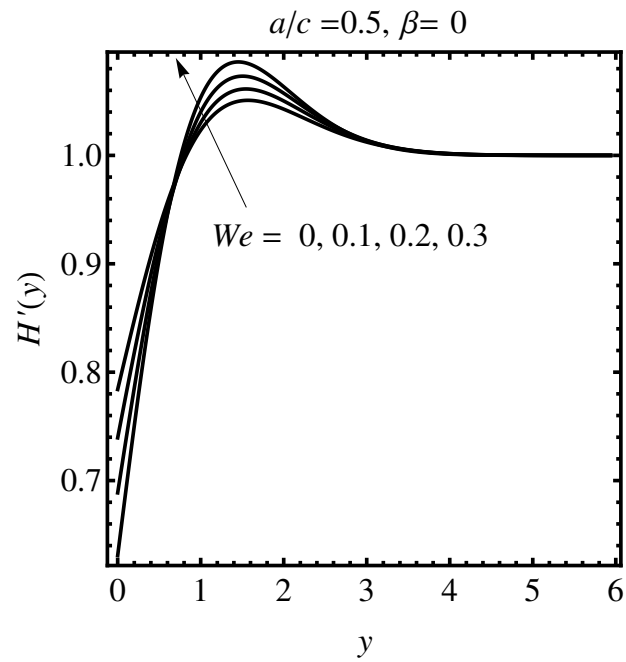


Figure 4.4: Effects of We on $H'(y)$ when $a/c = 0.5$.

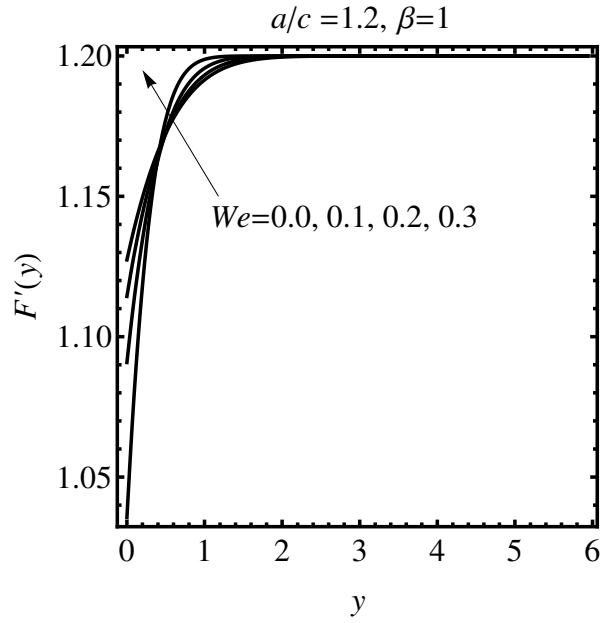


Figure 4.5: Effects of We on $F'(y)$ when $a/c = 1.2$ in the case of slip.

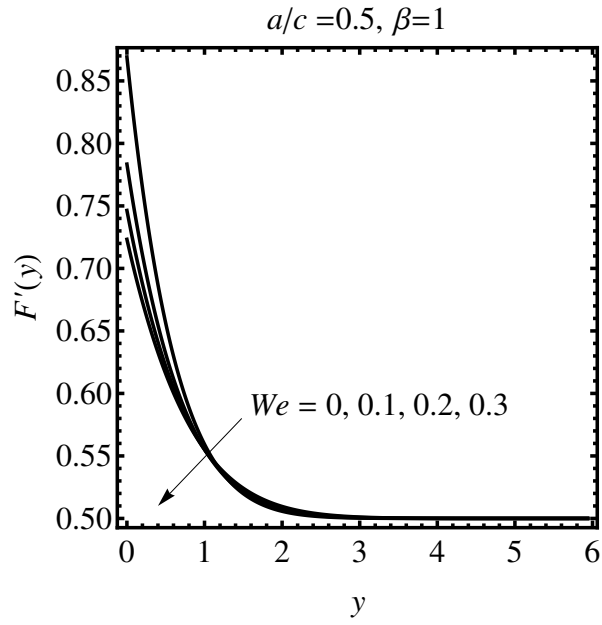


Figure 4.6: Effects of We on $F'(y)$ when $a/c = 0.5$ in the case of slip.

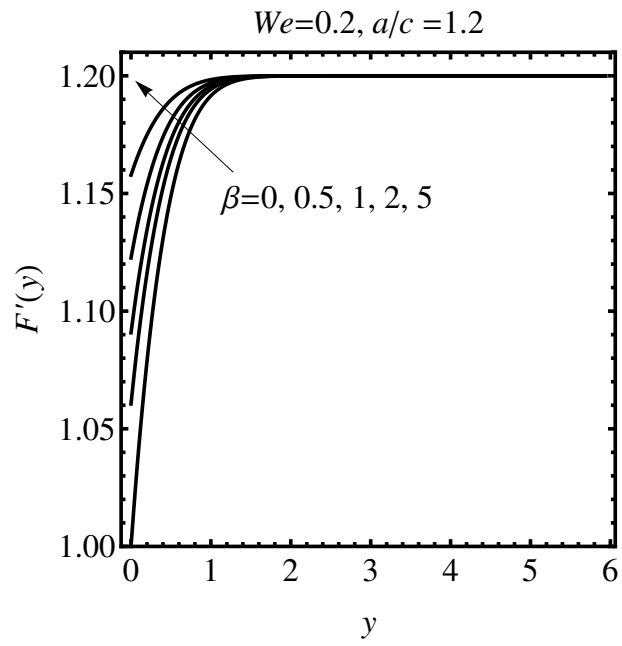


Figure 4.7: Effects of β on $F'(y)$ when $a/c = 1.2$.

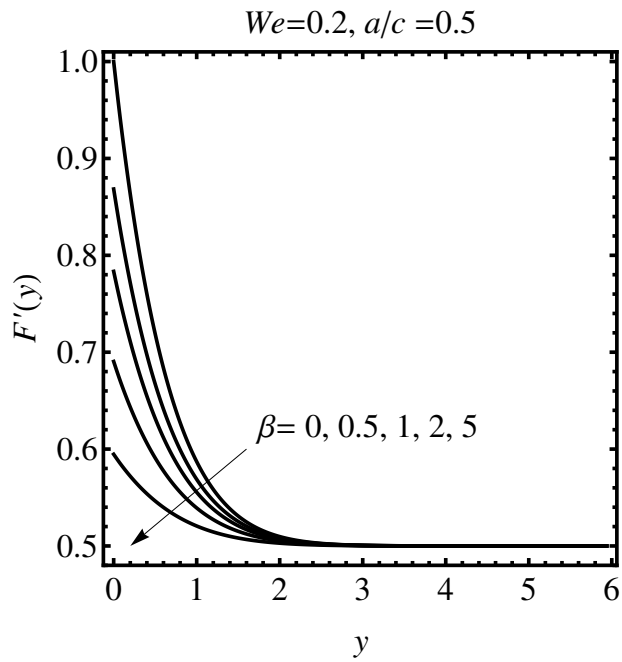


Figure 4.8: Effects of β on $F'(y)$ when $a/c = 0.5$.

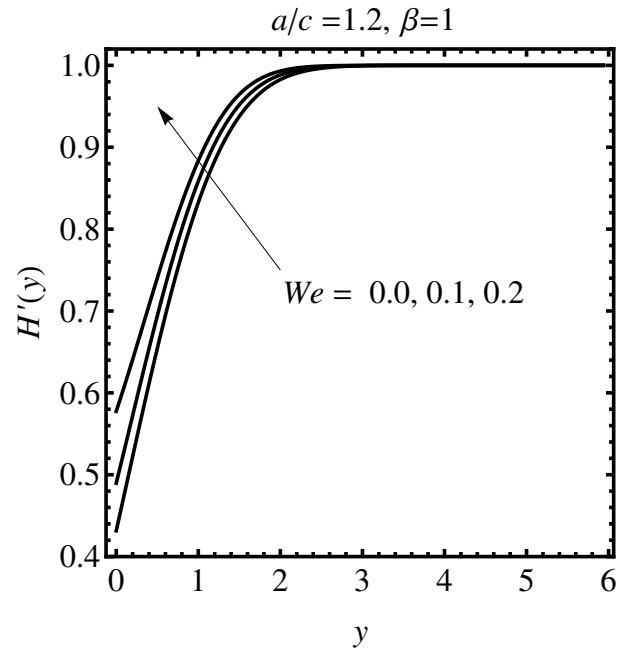


Figure 4.9: Effects of We on $H'(y)$ when $a/c = 1.2$ in the case of slip.

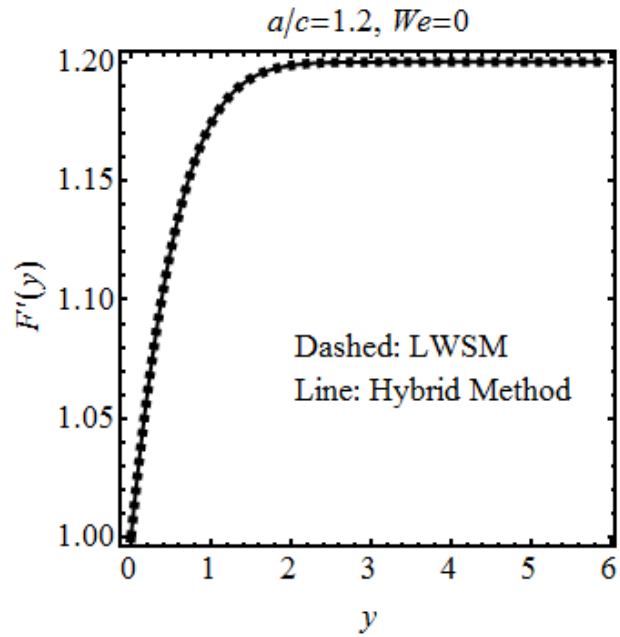


Figure 4.10: Comparison of methods for $We = 0.0$ when $a/c = 1.2$.

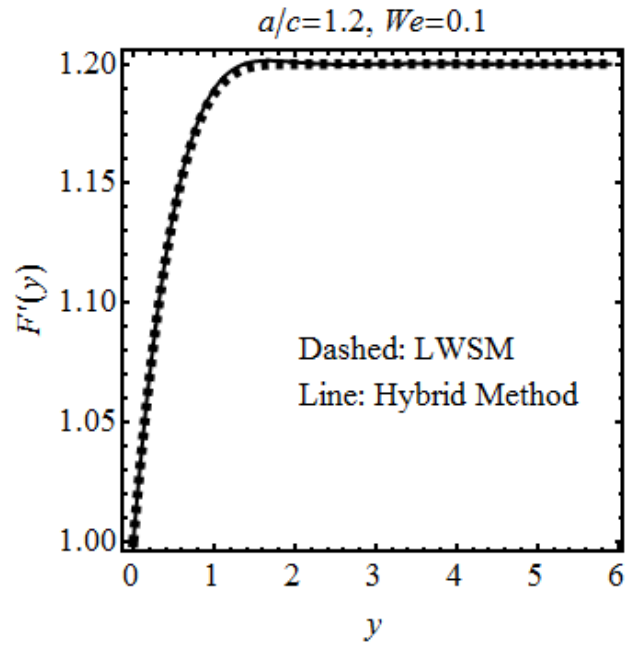


Figure 4.11: Comparison of methods for $We = 0.1$ when $a/c = 1.2$.

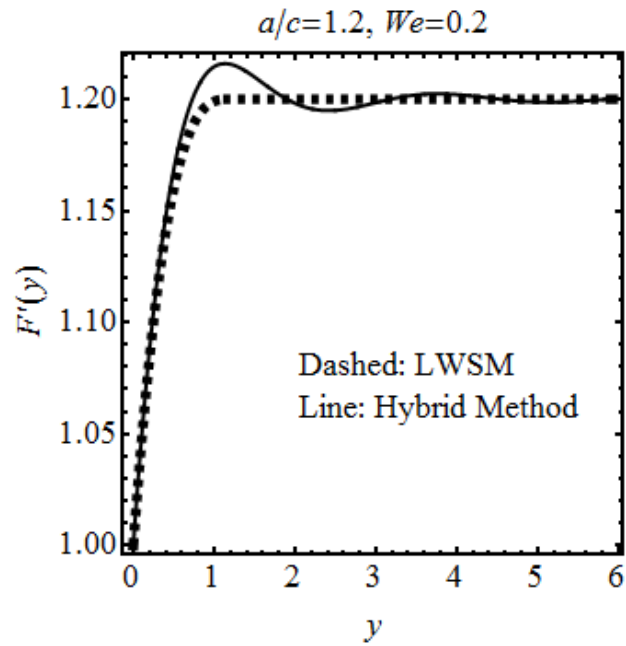


Figure 4.12: Comparison of methods for $We = 0.2$ when $a/c = 1.2$.

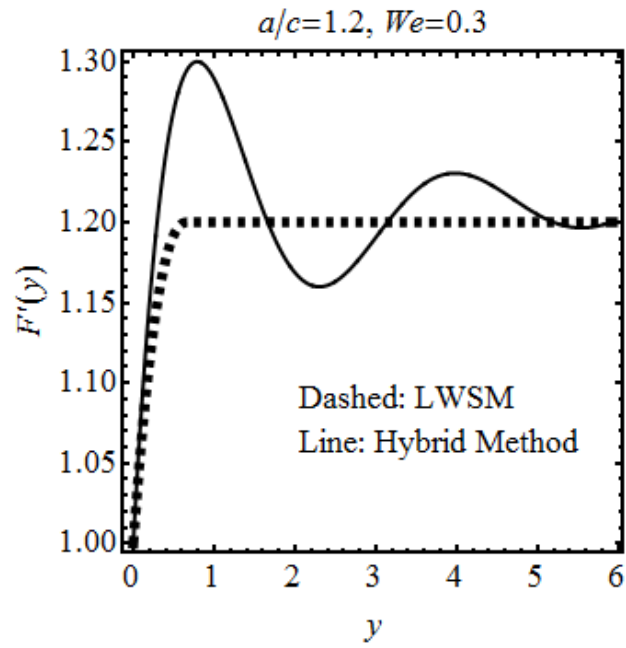


Figure 4.13: Comparison on methods for $We = 0.3$ when $a/c = 1.2$.

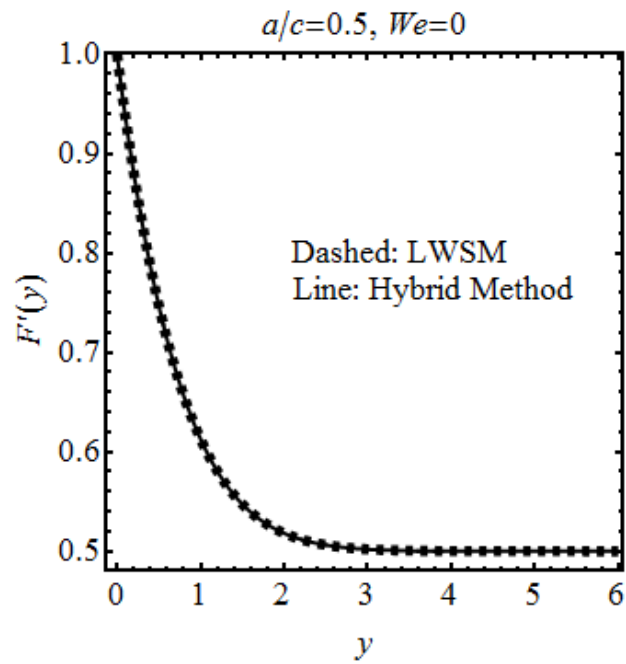


Figure 4.14: Comparison on methods for $We = 0.0$ when $a/c = 0.5$.

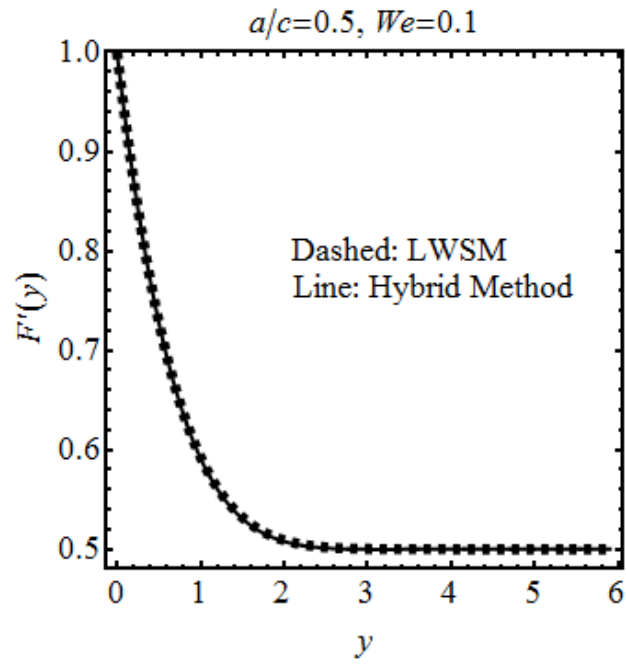


Figure 4.15: Comparison on methods for $We = 0.1$ when $a/c = 0.5$.

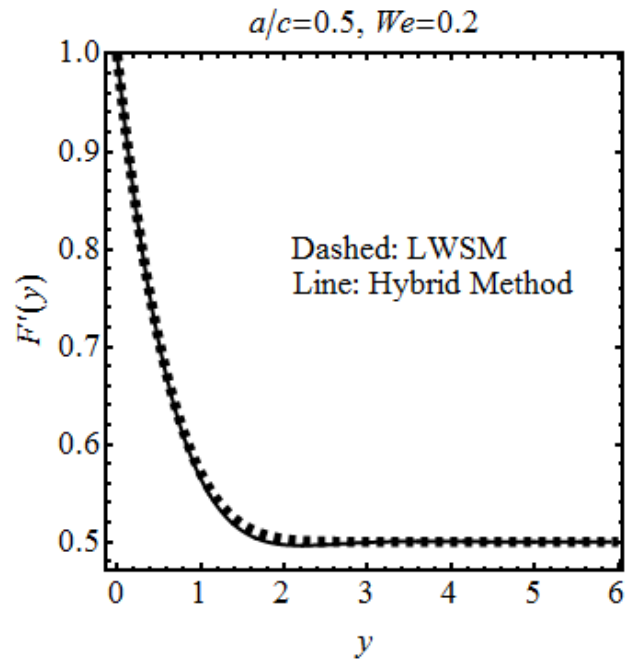


Figure 4.16: Comparison on methods for $We = 0.2$ when $a/c = 0.5$.

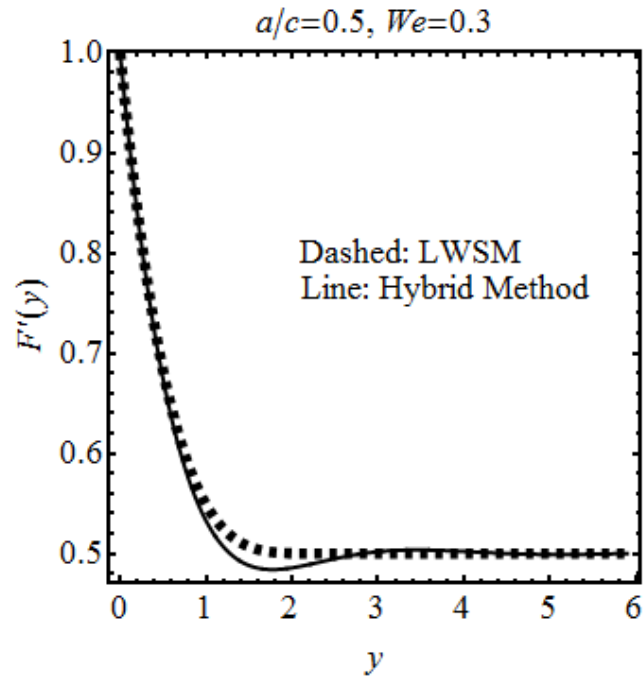


Figure 4.17: Comparison on methods for $We = 0.3$ when $a/c = 0.5$.

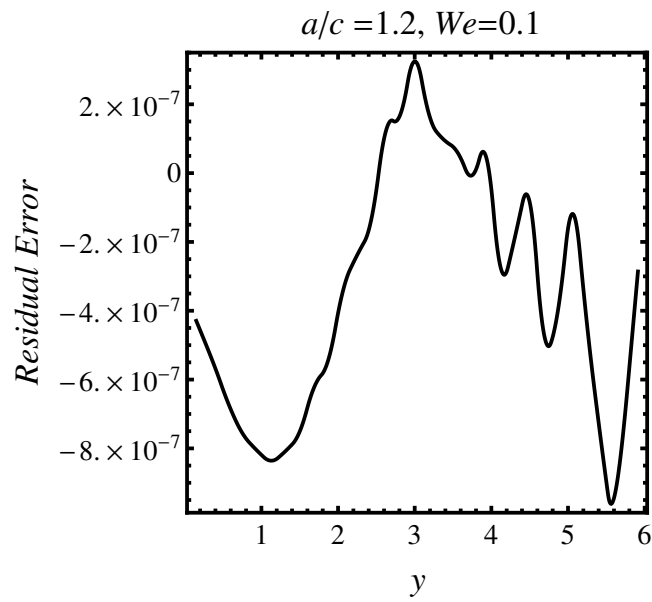


Figure 4.18: Graph of residual error for $We = 0.1$ and $a/c = 1.2$.

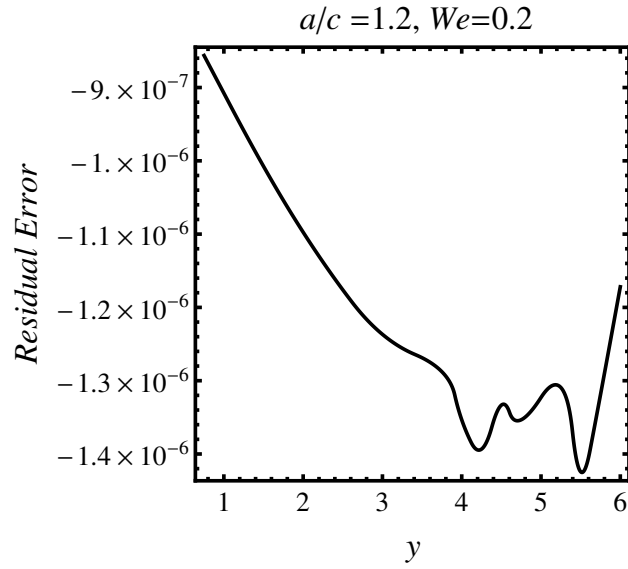


Figure 4.19: Graph of residual error for $We = 0.2$ and $a/c = 1.2$.

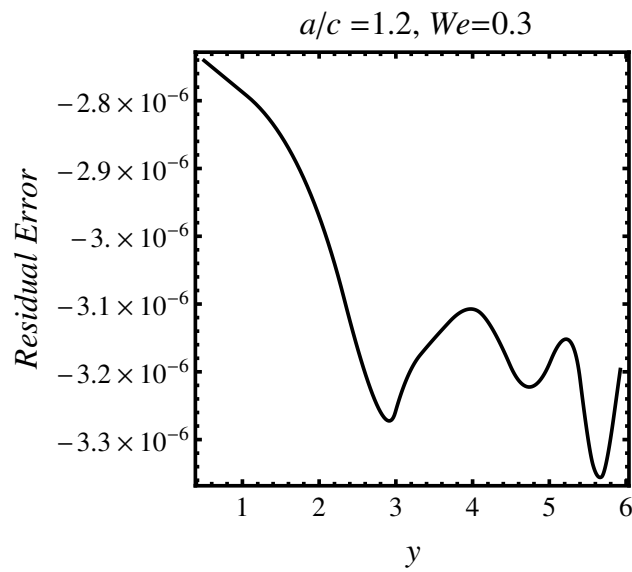


Figure 4.20: Graph of residual error for $We = 0.3$ and $a/c = 1.2$.

Chapter 5

Conclusions

The slip and radiation effects for the oblique stagnation-point flow over a stretching sheet for Walters-B fluid is investigated using two numerical techniques namely, a hybrid numerical method and a Legendre wavelet spectral collocation method. The main findings of current analysis are as under:

1. Increase in viscoelastic parameter We results in an increase in the velocity for the case $a/c > 1$ and decrease in velocity for the case $0 < a/c < 1$.
2. An increase in We enhances the temperature. The thermal boundary layer thickness is also increased.
3. Velocity of fluid increases by increasing stretching ratio parameter a/c .
4. Temperature and corresponding thermal boundary layer thickness decrease by increasing a/c .
5. Velocity and temperature increases for large values of slip.
6. An increase in effective Prandtl number Pr_{eff} diminishes the temperature and corresponding thermal boundary layer thickness.
7. An increase in λ increases the temperature and the corresponding thermal boundary layer thickness.

Bibliography

- [1] D.W. Beard and K. Walters, *Elastico-viscous boundary layer flows. I. Two-dimensional flow near a stagnation point*, Proc. Camb. Phil. Soc. 60 (1964) 667-674.
- [2] K.R. Frater, *On the solution of some boundary value problems arising in elasticoviscous fluid mechanics*, Z. Angew. Math. Phy. 21 (1970) 134-137.
- [3] P.D. Ariel, *A hybrid method for computing the flow of viscoelastic fluids*, Int. J. Numer. Meth. Fluids 14 (1992) 757-774.
- [4] P.D. Ariel, *Generalized Gear's method for computing the flow of viscoelastic fluids*, Comp. Meth. Appl. Mech. Eng. 142 (1997) 111-121.
- [5] J.M. Dorrepaal, O.P. Chandna, F. Labropulu, *The flow of a viscoelastic fluid near a point of reattachment*, Z. Angew. Math. Phy. 43 (1992) 708-714.
- [6] F. Labropulu, J.M. Dorrepaal, O.P. Chandna, *Viscoelastic fluid flow impinging on a wall with suction or blowing*, Mech. Res. Com. 20(2) (1993) 143-153.
- [7] F. Labropulu, M. Chinichian, *Unsteady oscillatory stagnation point flow of a viscoelastic fluid*, Int. J. Eng. Sci. 42 (2004) 625-633.
- [8] F. Labropulu, I. Hussain, M. Chinichian, *Stagnation point flow of Walters B fluid with slip*, Int. J. Math. Math. Sci. 61 (2004) 3249-3258.
- [9] D. Li, F. Labropulu, I. Pop, *Oblique stagnation point flow of a viscoelastic fluid with heat transfer*, Int. J. Non-Linear Mech. 44 (2009) 1024-1030.
- [10] F. Labropulu, D. Li, I. Pop, *non-orthogonal stagnation point flow towards a stretching surface in a non-Newtonian fluid with heat transfer*, Int. J. Ther. Sci. 49 (2010) 1042-1050.

- [11] I. Hussain, F. Labropulu, I. Pop, *Two dimensional oblique stagnation point flow towards a stretching surface in a viscoelastic fluid*, Cent. Eur. J. Phy. 9 (2011) 176-182.
- [12] C. Navier, *Memoire sur les lois du mouvement des fluids*, Mem. Acad. Sci. Inst. Fr. 6 (1827) 389-440.
- [13] M.A. Seddeek, M.S. Abdelmeguid, *Effects of radiation and thermal diffusivity on heat transfer over a stretching surface with variable heat flux*, Phy. Lett. A 348 (2006) 172-179.
- [14] A.K. Dizicheh, F. Ismail, M.T. Kajani, M. Maleki, *A Legendre wavelet spectral collocation method for solving oscillatory initial value problems*, J. App. Math. 2013 (2013) 591636.
- [15] T.Y. Na, *Computational methods in engineering boundary value problems*, Acad. Press, New York, (1979).
- [16] J.T. Stuart, *The viscous flow near a stagnation point when external flow has uniform vorticity*, J. Aero. Sci. 26 (1959) 124-125.
- [17] K.J. Tamada, *Two dimensional stagnation point flow impinging obliquely on a plane wall*, J. Phy. Soc. Jpn. 46 (1979) 310-311.
- [18] M. Dorrepaal, *An exact solution of Navier-Stokes equation which describes non-orthogonal stagnation point flow in two dimensions*, J. Fluid Mech. 163 (1986) 146-147.
- [19] R.C. Bataller, *Effects of heat source/sink, radiation and work done by deformation on flow and heat transfer of a viscoelastic fluid over a stretching sheet*, Comp. Math. Appl. 53 (2007) 305-316.
- [20] E. Magyari, A. Pantokratoras, *Note on the effect of thermal radiation in linearized Rosseland approximation on the heat transfer characteristics of various boundary layer flows*, Int. Commun. Heat Mass Transf. 38 (2011) 554-556.